iScience

CellPress
OPEN ACCESS

Article

TLR7 and IL-6 differentially regulate the effects of rotarod exercise on the transcriptomic profile and neurogenesis to influence anxiety and memory

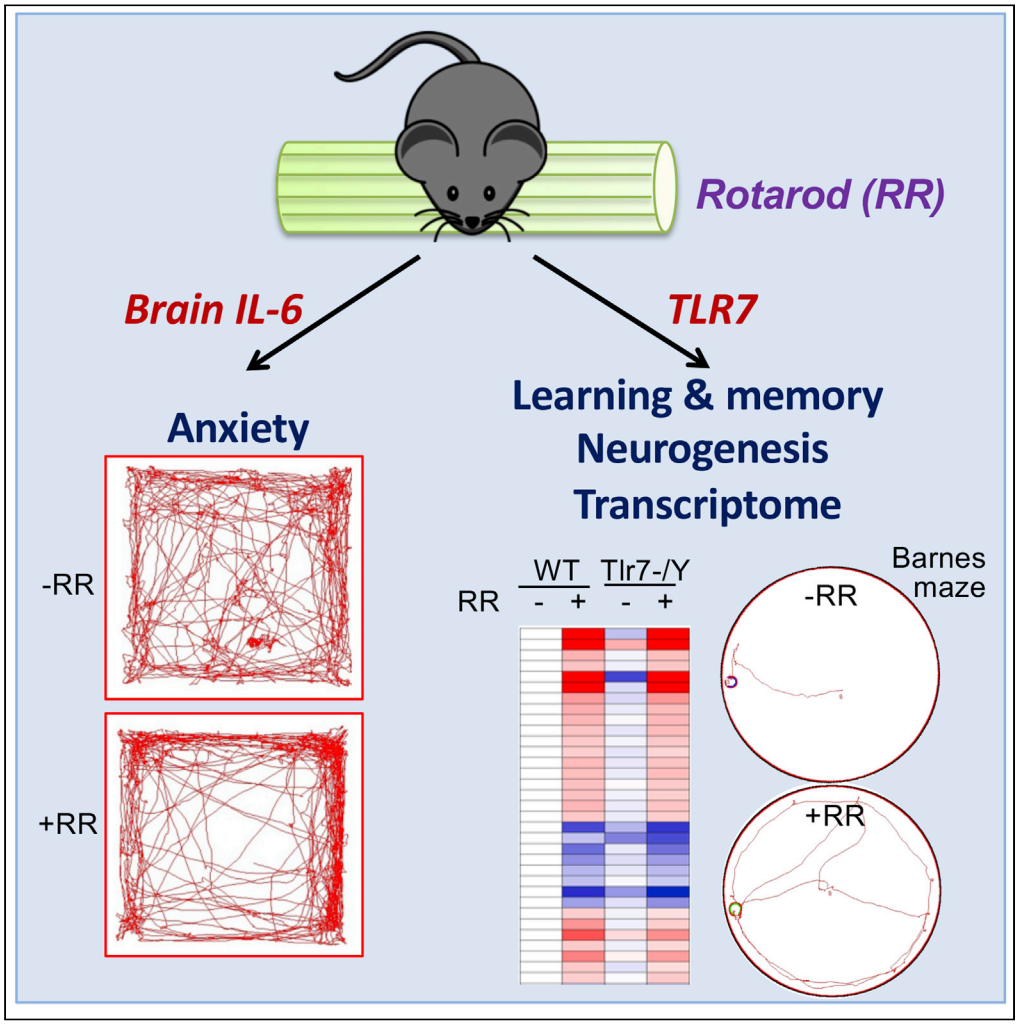

Yun-Fen Hung, Yi-Ping Hsueh

yph@gate.sinica.edu.tw

Highlights

Rotarod training at 5 or 10 weeks of age induces anxious behavior in an open field

Rotarod training upregulates IL-6 expression in the brain and results in anxiety

Rotarod training alters performances of test mice in spatial learning and memory

TLR7 controls the rotarod-impacted transcriptomic profiles and contextual memory

Hung & Hsueh, iScience *24*, 102384
April 23, 2021
https://doi.org/10.1016/j.isci.2021.102384

iScience

CellPress
OPEN ACCESS

Article

TLR7 and IL-6 differentially regulate the effects of rotarod exercise on the transcriptomic profile and neurogenesis to influence anxiety and memory

Yun-Fen Hung[1] and Yi-Ping Hsueh[1,2,*]

SUMMARY

Voluntary exercise is well known to benefit brain performance. In contrast, forced exercise induces inflammation-related stress responses and may cause psychiatric disorders. Here, we unexpectedly found that rotarod testing, a frequently applied assay for evaluating rodent motor coordination, induces anxiety and alters spatial learning/memory performance of mice. Rotarod testing upregulated genes involved in the unfolded protein response and stress responses and downregulated genes associated with neurogenesis and neuronal differentiation. It impacts two downstream pathways. The first is the IL-6-dependent pathway, which mediates rotarod-induced anxiety. The second is the Toll-like receptor 7 (TLR7)-dependent pathway, which is involved in the effect of rotarod exercise on gene expression and its impact on contextual learning and memory of mice. Thus, although rotarod exercise does not induce systemic inflammation, it influences innate immunity-related responses in the brain, controls gene expression and, consequently, regulates anxiety and contextual learning and memory.

INTRODUCTION

Exercise is known to influence brain functions in human and rodents (Delezie and Handschin, 2018; Pedersen, 2019). Voluntary exercise benefits neurogenesis and enhances the expression of neurotrophic factors to improve learning and memory performance (Bettio et al., 2019; Cooper et al., 2018; Hamilton and Rhodes, 2015; Pedersen, 2019; Rendeiro and Rhodes, 2018; Ryan and Nolan, 2016; Voss et al., 2019). However, for forced exercise, it is more complex because despite the beneficial effects provided by the muscular and cardiovascular systems, forced exercise (such as treadmills for rodents) also can induce stress responses (Contarteze et al., 2008; Svensson et al., 2016) and systemic inflammation (Cook et al., 2013; Nambot et al., 2020). Stress triggers the unfolded protein response of the ER(Gold et al., 2013; Hotamisligil, 2010), influences neural plasticity (Duman and Li, 2012; Pittenger and Duman, 2008) and neurogenesis (De Miguel et al., 2019), and it decreases dendritic spine density and shortens the dendritic branches of neurons (De Miguel et al., 2019). Consequently, forced exercise impairs spatial memory (de Quervain et al., 2017) and results in anxiety (Gold et al., 2015). Thus, the stress condition caused by forced exercise damages the brain function, although the detailed mechanism remained unclear.

Toll-like receptors (TLR) detect both exogenic pathogenic pattern molecules and endogenous damage signals to trigger innate immune responses. Consequently, in addition to removing pathogens, TLR activation also fine-tunes organ development and morphogenesis (Akira and Sato, 2003; Chen et al., 2019; Kumar et al., 2009; Liu et al., 2014; Sommer and Bäckhed, 2013). For instance, activation of TLR3 or TLR4 by systemic administration of poly(I:C) or lipopolysaccharide at prenatal or neonatal stages, respectively, results in anxiety and other behavioral defects similar to the features of neurodevelopmental disorders (Bilbo et al., 2018; Chen et al., 2019; Khandaker et al., 2015; Knuesel et al., 2014). TLRs are also involved in sensing gut microbiota to modulate homeostasis and development of host immune and gastrointestinal systems, as well as influencing metabolism, development and brain function (Burgueño and Abreu, 2020; Caputi and Giron, 2018; Lin et al., 2019; Sommer and Bäckhed, 2013; Spiljar et al., 2017; Yiu et al., 2017). Deletion of TLRs also alters mouse behaviors (Chen et al., 2019; Hung et al., 2018a; Liu et al., 2013), strengthening evidence for the roles of TLRs in regulating brain function.

[1]Institute of Molecular Biology, Academia Sinica, Taipei 11529, Taiwan, ROC

[2]Lead contact

*Correspondence: yph@gate.sinica.edu.tw

https://doi.org/10.1016/j.isci.2021.102384

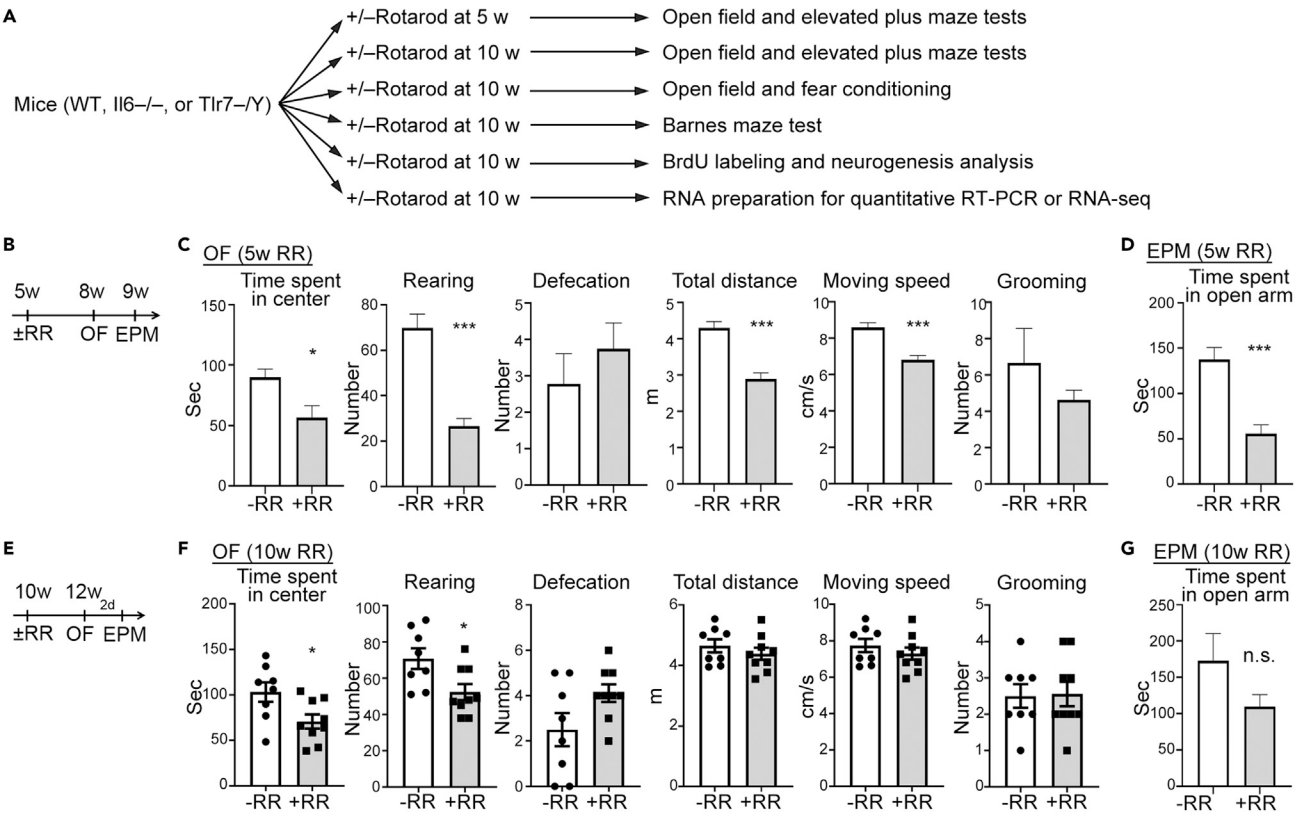

Figure 1. Rotarod training at 5 or 10 weeks of age induces anxiety in adult mice

(A) Outline of our experimental design.

(B) Arrangement of behavioral paradigms for (C and D). A rotarod test (RR) was carried out on mice at 5 weeks (w) of age, followed by open field (OF) and elevated plus maze (EPM) as indicated.

(C) The results of open field test on mice with rotarod training at 5 weeks of age.

(D) The results of elevated plus maze test of mice with rotarod training at 5 weeks of age (n = 9 for WT–RR, n = 8 for WT + RR).

(E) Arrangement of behavioral paradigms for (F)-(G). Mice were subjected to rotarod training at 10 weeks of age.

(F) The results of open field test on mice with rotarod training at 10 weeks of age.

(G) The results of elevated plus maze test on mice with rotarod training at 10 weeks of age (n = 8 for WT–RR mice, n = 9 for WT + RR mice).

Data represent mean plus SEM. Two-tailed Mann-Whitney U test (B-C). *$p < 0.05$; ***$p < 0.001$.

In this study, we report that rotarod testing, a popular exercise assay for assessing the motor coordination and balance of rodents, induces anxiety and alters spatial learning/memory of mice. Using genetically modified mice, we demonstrate that rotarod training uses IL-6 and TLR7 pathways to regulate neurogenesis and transcription and thereby controls various mouse behaviors. Our study dissects mechanistic details of how innate immune molecules control behaviors and brain plasticity, and it also suggests that rotarod testing can interfere with other brain functions, such as emotion and learning/memory.

RESULTS

Rotarod training induces anxious behaviors

To characterize the behavioral features of mice, the same mice were usually subjected to a series of behavioral paradigms. We unexpectedly found that accelerating rotarod test likely influenced the results of behavioral assays following the rotarod test. It seems that the accelerating rotarod test with three trials per day for three consecutive days can change brain activity and function and therefore alter the performance of mice in other behavioral tests. To investigate this possibility, we subjected naive mice to a rotarod test on three consecutive days at the ages of 5 or 10 weeks (Figure 1A). Data on animal usage for each experiment are available in Table S1. Mouse performance in rotarod testing is summarized in Figure S1. After rotarod training, various behavioral tests, immunostaining, quantitative RT-PCR and transcriptomic

analyses were applied to establish if and how rotarod training influences brain function and plasticity (Figure 1A). First, we characterized mice subjected to rotarod training at the age of 5 weeks (Figure 1B). Compared with mock control mice, 5-week-old mice that underwent rotarod training spent less time in the central area and exhibited a reduced number of rearing events and lower overall moving distance and speed in the open field assay (Figure 1C). Mice treated with rotarod training at 5 weeks old also spent less time exploring the open arm of an elevated plus maze (Figure 1D). These results suggest that rotarod treatment at the age of 5 weeks impairs both horizontal and vertical movements and induces anxious behavior in mice at the age of 8–9 weeks. For mice subjected to the rotarod test at the age of 10 weeks (Figure 1E), they still spent less time in the central area of the open field and presented fewer rearing events (Figure 1F). However, although rotarod training at the age of 10 weeks tended to reduce the time spent exploring the open arm of an elevated plus maze, the difference relative to control was not significant (Figure 1G). Thus, compared to juvenile mice, adult mice were relatively resistant to rotarod treatment, but still exhibited abnormal behaviors in an open field.

Note, for our 5-week-old mice cohort, some of the mice tended to jump away from the moving rod at day 3 of rotarod training, consequently shortening the time they stayed on the rod (Figure S1A). Ten-week-old mice exhibited normal motor learning ability to stay on the rotarod longer when they received more training trials (Figure S1B). It is unclear why some of the 5-week-old mice tended to jump away from the rotarod. It may be due to hyperactivity at the adolescence stage or hypersensitivity to the duress of rotarod testing. Since 10-week-old mice behaved much more stably than 5-week-old mice on the rotarod, we used 10-week-old mice in the following experiments.

IL-6 is involved in rotarod-induced anxiety

To further confirm and characterize rotarod-induced anxiety in adult mice, we used quantitative RT-PCR (Table S2) to analyze cytokine expression in cortices, hippocampi and spleens 3 hr after undergoing rotarod treatment at the age of 10 weeks. In this report, we always mixed cortical and hippocampus tissues to represent RNA samples prepared from brains. Among the five cytokines we examined (i.e., IL-6, IL-1β, TNFα, IFNβ and CCL5), we found that mRNA levels of *Il6* were increased in brains of adult WT mice that undertook rotarod training (Figure 2A, upper) but not in their spleens (Figure 2A, lower). In fact, mRNA levels of both *Il6* and *Il1β* tended to be reduced in the spleen of adult WT mice following rotarod training (Figure 2A, lower). Thus, rotarod training specifically induced *Il6* expression in brains among examined cytokines. Although *Il6* levels in the brain were increased, the population of glial cells was not altered by rotarod training (Figure S2, both microglia and astrocytes). Expression of various *Tlr* genes in both brains and spleens was also not influenced by rotarod training (Figure S3). These results suggest that although the rotarod assay induces expression of IL-6 in cortices and hippocampi, the effect of rotarod testing on inflammation was not global. Rotarod training did not induce noticeable inflammation in peripheral tissues.

To evaluate the role of IL-6 in rotarod-induced anxiety, we subjected *Il6* knockout mice to rotarod training. Unlike adult WT mice, $Il6^{-/-}$ mice pretrained with a rotarod assay did not spend more time in corners of an open field test and rearing behavior was not affected (Figure 2B). Numbers of glial cells were also unaltered (Figures 2C and 2D, information on antibodies is available in Table S3).

Taken together, these results suggest that IL-6 is critical for rotarod-induced anxiety in an open field test, and that glial cells are not involved in the effect of rotarod training on adult mice.

TLR7 is not involved in rotarod-induced anxiety

Next, we tested *Tlr7* knockout mice for rotarod-induced stress responses because our previous studies have shown that TLR7 activation in neurons induces IL-6 expression to control neuronal morphology (Liu et al., 2013) and that *Tlr7* knockout mice (i.e. $Tlr7^{-/y}$ mice) are less anxious and perform normally in rotarod test (Hung et al., 2018a) Since *Il6* is critical for rotarod-induced anxiety (Figure 1D), we investigated if TLR7 is involved in that response. Consistent with our previous study, *Tlr7* deletion did not influence the results of rotarod testing (Figure S1D). Similar to WT mice, *Il6* RNA levels were still upregulated in $Tlr7^{-/y}$ mouse cortices and hippocampi after rotarod training, although reduced *Il6* expression was found in the spleen of $Tlr7^{-/y}$ mice (Figure 2A). This result suggests that TLR7 is unlikely involved in rotarod-induced *Il6* expression. In the open field, $Tlr7^{-/y}$ mice subjected to rotarod training ($Tlr7^{-/y}$ + RR) also spent less time in the central area and longer in the corners, which is a similar outcome to rotarod-trained WT mice (WT + RR)

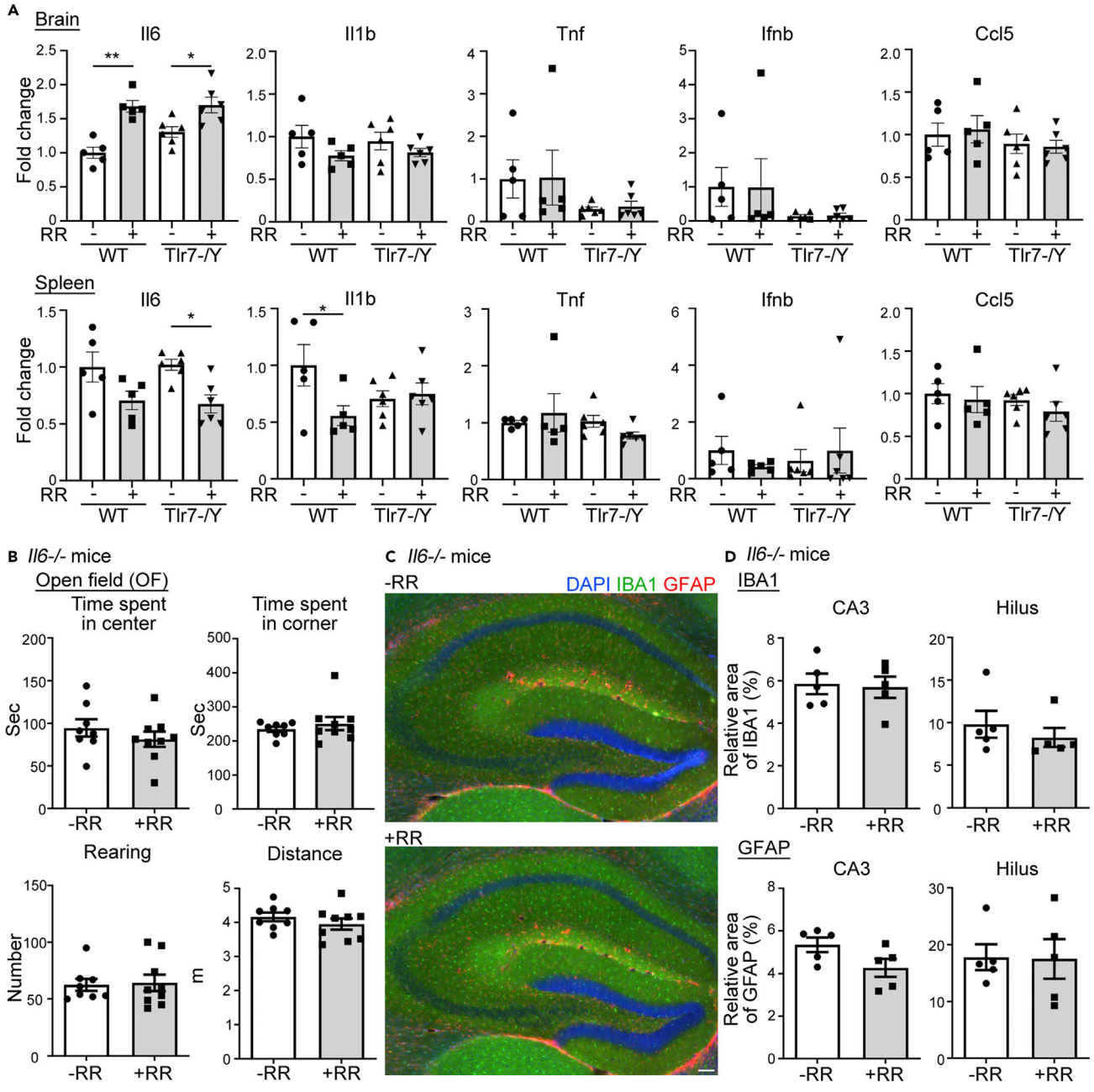

Figure 2. Rotarod training at 10 week of age induces anxiety through IL-6

(A) Rotarod training at 10 weeks of age differentially regulates cytokine expression in brain tissue (cortices and hippocampi) and spleens. Quantitative PCR was performed to measure relative cytokine expression levels in WT and *Tlr7*$^{-/y}$ mice (n = 5 for WT, n = 6 for *Tlr7*$^{-/y}$).

(B) Deletion of *Il6* mitigates rotarod-induced anxiety in an open field (n = 8 for *Il6*$^{-/-}$–RR mice, n = 9 for *Il6*$^{-/-}$+RR mice).

(C) Rotarod training does not alter the population of glial cells in hippocampi (n = 5 for ± RR). Representative images of GFAP (red) and IBA1 (green) dual staining are shown.

(D) Quantification of IBA1 and GFAP immunoreactivities. Signal coverage (area) percentage of the CA3 and hilus regions of hippocampi was determined. Data represent mean +/− SEM and the results of individual samples are shown. Two-tailed Mann-Whitney U test (B and D); two-way ANOVA with Bonferroni's multiple comparisons test (A). *, $p < 0.05$; **, $p < 0.01$. Scale bar: (C) 100 μm.

(Figures 3A (1) and 3B). However, in contrast to WT mice, rotarod training did not reduce the number of rearing events of *Tlr7*$^{-/y}$ mice in the open field (Figure 3B, *Tlr7*$^{-/y}$–RR vs. *Tlr7*$^{-/y}$ + RR). Thus, *Tlr7* deletion influences some but not all rotarod-induced behavioral alterations in the open field.

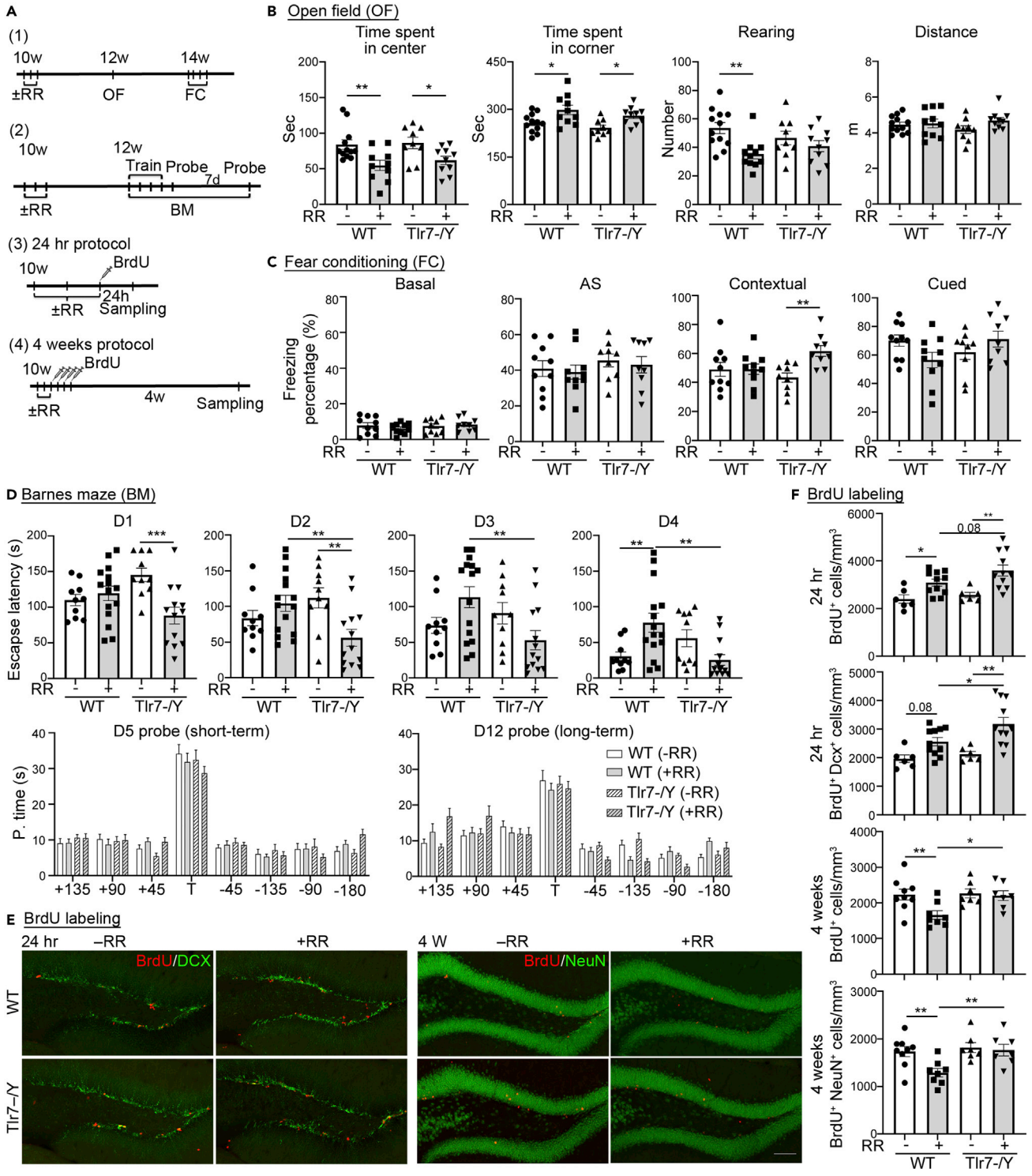

Figure 3. *Tlr7* deletion alters rotarod-induced behavioral patterns and neurogenesis

(A) Experimental arrangements for mice with rotarod training at 10 weeks of age. (1) for (B) and (C); (2) for (D); (3) and (4) for (E) and (F).

(B) The effect of rotarod training (RR) on open field (OF) responses. Rotarod training reduced the time spent in the center of an open field for both WT and *Tlr7*$^{-/y}$ mice, but not the number of rearing events of *Tlr7*$^{-/y}$ mice (n = 12 for WT–RR, n = 10 for WT + RR, n = 9 for *Tlr7*$^{-/y}$–RR, n = 10 for *Tlr7*$^{-/y}$ + RR).

(C) The effect of RR on fear conditioning. Rotarod training solely enhanced contextual memory of *Tlr7*$^{-/y}$ mice (n = 10 for WT ± RR, n = 9 for *Tlr7*$^{-/y}$ ± RR). AS, right after stimulation (representing pain sensation).

Figure 3. *Continued*

(D) In Barnes maze, RR differentially impacted escape latency in WT and *Tlr7*$^{-/y}$ mice but did not affect short- (D5) or long-term (D12) memory (n = 10 for WT–RR, n = 15 for WT + RR, n = 10 for *Tlr7*$^{-/y}$–RR, n = 13 for *Tlr7*$^{-/y}$ + RR).

(E) Representative images of BrdU labeling.

(F) The results of BrdU labeling. For short-term 24-hr BrdU labeling, RR enhanced neurogenesis in both WT and *Tlr7*$^{-/y}$ mice (n = 6 for WT–RR, n = 11 for WT + RR, n = 6 for *Tlr7*$^{-/y}$–RR, n = 11 for *Tlr7*$^{-/y}$ + RR). For long-term 4-week BrdU labeling, RR reduced neural differentiation only in WT mice but not in *Tlr7*$^{-/y}$ mice (n = 9 for WT–RR, n = 8 for WT + RR, n = 7 for *Tlr7*$^{-/y}$–RR, n = 7 for *Tlr7*$^{-/y}$ + RR).

Data represent mean +/− SEM and the results of individual samples are shown. two-way ANOVA with Bonferroni's multiple comparisons test (B–D and F). *, $p < 0.05$; **, $p < 0.01$. Scale bar: (E) 100 μm.

Rotarod training differentially regulates contextual learning and memory in WT and *Tlr7*$^{-/y}$ mice

We then investigated if rotarod training influences the outcomes of fear conditioning and Barnes maze assays in WT and *Tlr7*$^{-/y}$ mice (Figure 3A (1)-(2)). The fear conditioning assay tested both contextual and cued fear memory. For WT mice, we did not observe an effect of rotarod training on contextual or cued fear memory. However, we did find that the performance of *Tlr7*$^{-/y}$ mice in contextual fear memory was enhanced after rotarod treatment (Figure 3C).

For the Barnes maze test, mice underwent four training trials to find an escape hole every day for four consecutive training days (D1-D4), and were then subjected to a short-term memory test at D5 and a long-term memory test at D12. We found that the rotarod treatment impaired the learning performance of WT mice, as the WT + RR group took much longer to find the escape hole at D4 (Figure 3D, upper). The learning performance of the *Tlr7*$^{-/y}$–RR group was similar to that of the WT–RR group (Figure 3D, upper, D4). Consistent with their better performance in contextual fear memory, *Tlr7*$^{-/y}$ + RR mice took less time to find the escape hole than non-rotarod-trained counterparts (i.e. *Tlr7*$^{-/y}$–RR) at D1 and D2 or the WT + RR group from D2 to D4 (Figure 3D, upper). Performances of these four groups in both short-term and long-term memory tests were similar to each other (Figure 3D, lower).

Together, the results of our fear conditioning and Barnes maze tests demonstrate that rotarod pretreatment may impair the spatial learning ability of WT mice but can enhance the spatial learning performance of *Tlr7*$^{-/y}$ mice, indicating that *Tlr7* deletion alters the response of mice to rotarod training, especially with regard to spatial learning.

Rotarod training differentially enhances neurogenesis and neural differentiation in WT and *Tlr7*$^{-/y}$ mice

Next, we investigated the effect of rotarod training on neurogenesis and differentiation of the hippocampal dentate gyrus (Figure 3A (3) and (4)). After the last day of rotarod training, we intraperitoneally injected bromodeoxyuridine (BrdU) into mice to label newborn neurons. Twenty-four hours after BrdU treatment, we observed that numbers of BrdU + cells were increased in both WT and *Tlr7*$^{-/y}$ mice with rotarod training (Figures 3E and 3F). The majority of those BrdU + cells were also doublecortin (DCX)-positive (Figures 3E and 3F), confirming that BrdU labeled newly generated neurons. Thus, neurogenesis was enhanced by rotarod training in both WT and *Tlr7*$^{-/y}$ mice. However, when we performed BrdU staining 4 weeks later (Figure 3A (4)), we found that the WT + RR group presented reduced numbers of BrdU + cells and BrdU + NeuN + cells compared with the other three groups (Figures 3E and 3F). Since NeuN labels differentiated neurons (Gusel'nikova and Korzhevskiy, 2015), these results suggest that although rotarod training promoted neurogenesis in WT mice, the newborn neurons could not differentiate and integrate into the brain circuitry. In contrast, numbers of both BrdU + cells and BrdU + NeuN + cells of the *Tlr7*$^{-/y}$ + RR group were comparable to those of the WT–RR and *Tlr7*$^{-/y}$–RR groups (Figures 3E and 3F). Together, these data suggest that *Tlr7* deletion neutralizes the negative effect of rotarod training on neural differentiation.

Rotarod training differentially alters the transcriptomic profiles of WT and *Tlr7*$^{-/y}$ mice

To characterize the molecular features of rotarod-induced stress and the effect of *Tlr7* knockout, we analyzed the transcriptomic profiles of the WT–RR, WT + RR, *Tlr7*$^{-/y}$–RR and *Tlr7*$^{-/y}$ + RR groups. Four mice were used for each group. Three hours after undergoing rotarod training or mock control, total RNA was isolated from mouse cortices and hippocampi and analyzed using RNA-seq. Principle component analysis (PCA) indicated that rotarod training indeed elicits differential gene expression in WT and *Tlr7*$^{-/y}$ mouse brains (Figure 4A). Based on criteria of fold-change > 1.3, a false discovery rate <0.1 and average

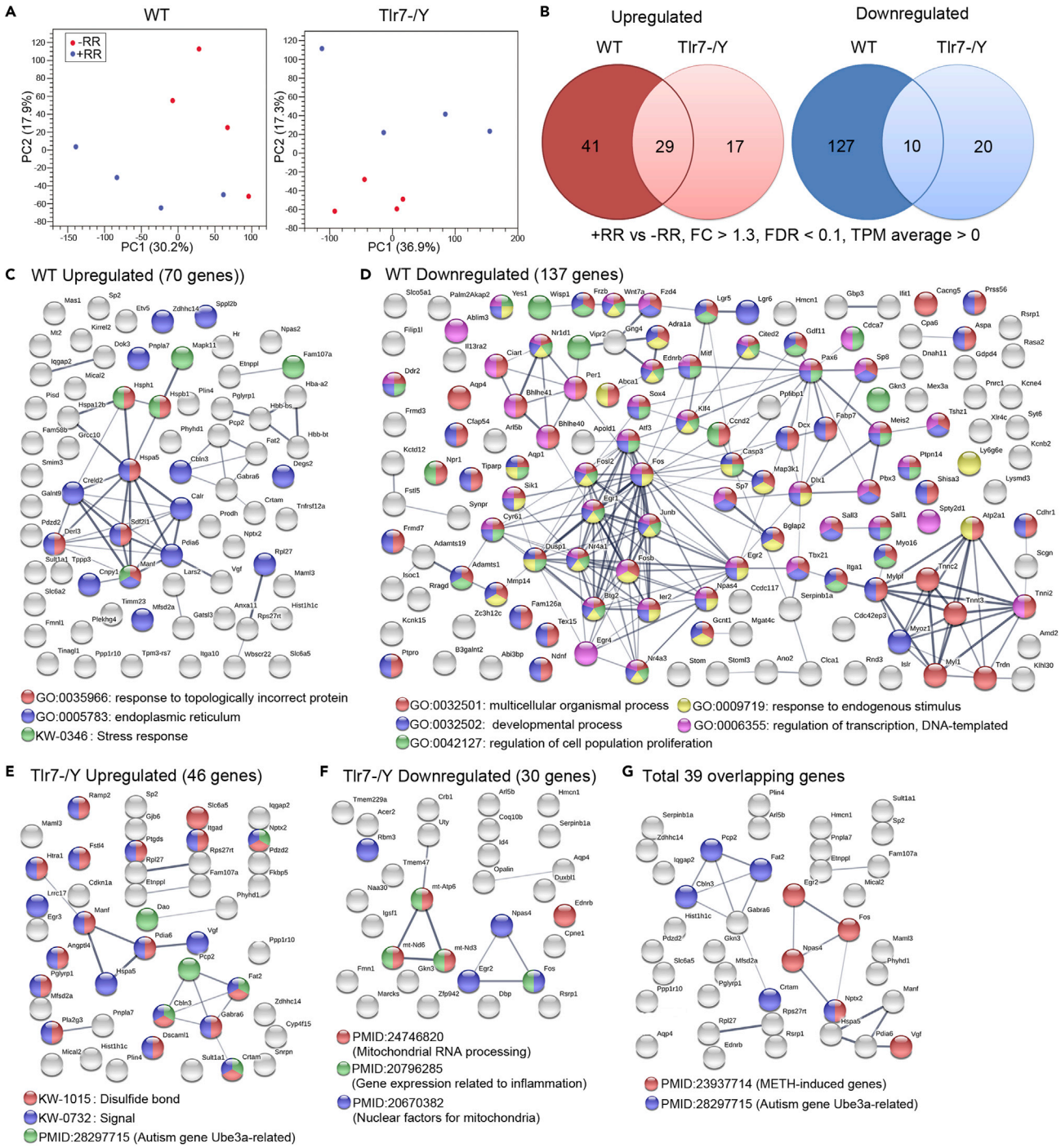

Figure 4. Transcriptomic profiles and networks are differentially altered by rotarod training in WT and *Tlr7*$^{-/y}$ mice

(A) Principal component analysis of RNA-seq data from WT and *Tlr7*$^{-/y}$ mouse brains with/without rotarod training.

(B) Venn diagram showing overlap of upregulated (left) and downregulated (right) genes between WT and *Tlr7*$^{-/y}$ mice following rotarod training. Gene lists are provided in Tables S1 and S2. FC, fold-change; FDR, false discovery rate; TPM, transcripts per million.

(C–G) Protein interaction networks analyzed by STRING. Node color represents an association with the different networks indicated at the bottom. Nodes with multiple colors indicate associations with multiple networks.

A

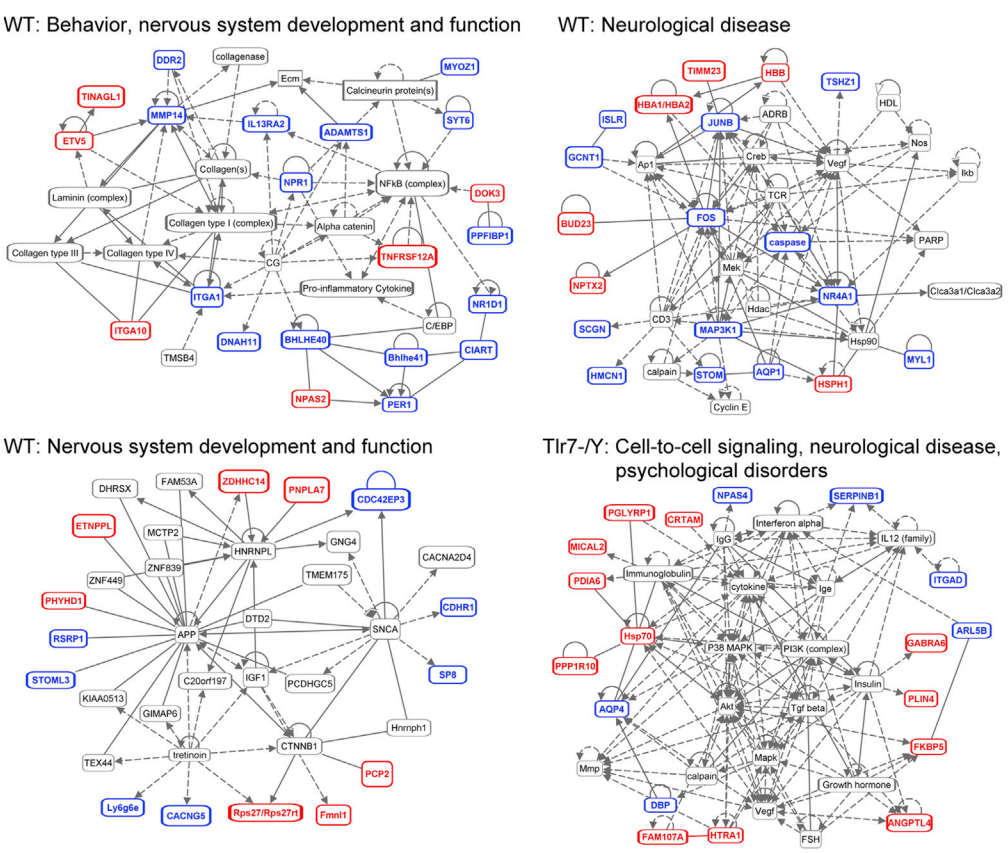

B

	Gene	Reference Title	PMID
Up (18/29)	Nptx2	NPTX2 is a key component in the regulation of anxiety	29844474
	Plin4	Investigation of the underling mechanism of ketamine for antidepressant effects in treatment-refractory affective disorders via molecular profile analysis	31281445
	Pdia6	The DNA methylome in panic disorder: a case control and longitudinal psychotherapy-epigenetic study	31754096
	Drr1	Tumor suppressor down-regulated in renal cell carcinoma 1 (DRR1) is a stress-induced actin bundling factor that modulates synaptic efficacy and cognition	21969592
	Sult1a1	Effects of antidepressant drug exposure on gene expression in the developing cerebral cortex	24458505
	Hspa5	Behavioral and Proteomic Analysis of Stress Response in Zebrafish (Danio rerio)	25398274
	Pdzd2	Genome-wide association study of comorbid depressive syndrome and alcohol dependence	22064162
	Mical2	A Systems Approach Identifies Networks and Genes Linking Sleep and Stress: Implications for Neuropsychiatric Disorders	25921536
	Hist1h1c	Distinctive gene expression profile in women with history of postpartum depression	27816578
	Gabra6	A new stress sensor and risk factor for suicide: the T allele of the functional genetic variant in the GABRA6 gene	29018204
	Pcp2	Sex-dependent behavioral functions of the Purkinje cell-specific Gαi/o binding protein, Pcp2(L7)	22528962
	Ppp1r10	Acute and chronic stress differentially regulate cyclin-dependent kinase 5 in mouse brain: implications to glucocorticoid actions and major depression	26057048
	Zdhhc14	Further evidence for linkage of bipolar disorder to chromosomes 6 and 17 in a new independent pedigree series	22329474
	Vgf	VGF function in depression and antidepressant efficacy	29158577
	Mfsd2a	Mfsd2a is a transporter for the essential omega-3 fatty acid docosahexaenoic acid	24828044
	Slc6a5	Expression of cerebral serotonin related to anxiety-like behaviors in C57BL/6 offspring induced by repeated subcutaneous prenatal exposure to low-dose lipopolysaccharide	28650979
	Etnppl	Shared gene expression alterations in schizophrenia and bipolar disorder	18191109
	Phyhd1	Transcriptome-Wide Expression Profiling in Skin Fibroblasts of Patients with Joint Hypermobility Syndrome/ Ehlers-Danlos Syndrome Hypermobility Type	27518164
Down (8/10)	Npas4	Effects of Npas4 deficiency on anxiety, depression-like, cognition and sociability behaviour	25549857
	Egr2	Genetic association of the EGR2 gene with bipolar disorder in Korea	22089088
	Fos	Convergent functional genomics of anxiety disorders: translational identification of genes, biomarkers, pathways and mechanisms	22832404
	Gkn3	Genetic Factors Mediate the Impact of Chronic Stress and Subsequent Response to Novel Acute Stress	22832404
	Aqp4	Requirement of AQP4 for Antidepressive Efficiency of Fluoxetine: Implication in Adult Hippocampal Neurogenesis	18923397
	Ednrb	Amygdalar Endothelin-1 Regulates Pyramidal Neuron Excitability and Affects Anxiety	28539637
	Hmcn1	HMNC1 gene polymorphism associated with postpartum depression	24604465
	Rsrp1	Activity-dependent aberrations in gene expression and alternative splicing in a mouse model of Rett syndrome	29769330

C

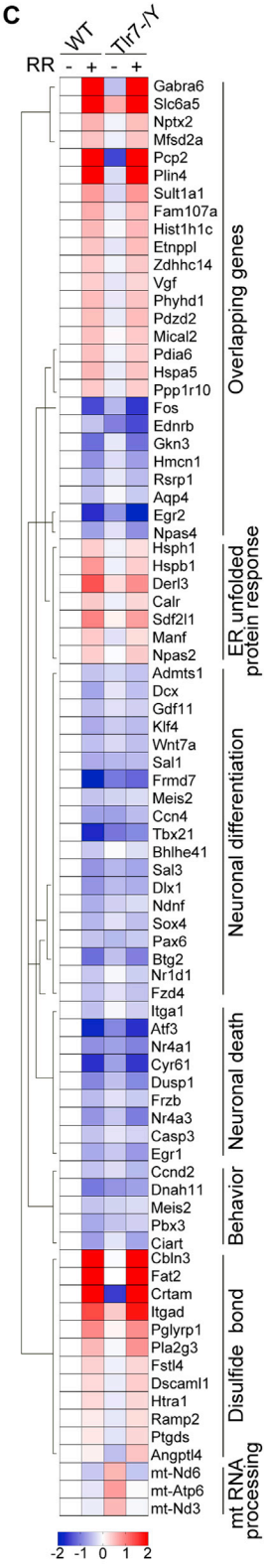

Figure 5. Genes regulated by rotarod training are highly correlated with neurological functions and diseases

(A) Ingenuity Pathway Analysis (IPA) of genes regulated by rotarod training in WT and *Tlr7*$^{-/y}$ mouse brains. Both upregulated (red) and downregulated (blue) genes were combined for IPA. The functions of each network are indicated. Black font depicts genes unaffected by rotarod training but that interact with identified differentially expressed genes (DEG).

(B) Overlapping DEG are highly relevant to anxiety. Eighteen and eight genes out of a total of 29 upregulated and 10 downregulated genes, respectively, are associated with anxiety. The related manuscripts and their PMIDs are indicated.

(C) Heatmap of DEG. Color intensity represents relative TPM levels (log2 values) normalized to the WT–RR group. Gene groupings are also indicated. The color-coded bar represents the *Z* score.

transcripts per million (TPM) > 0 (in each group), we identified 70 upregulated and 137 downregulated genes in WT brains (Figure 4B, Table S4). For *Tlr7*$^{-/y}$ mice, 46 and 30 up- and downregulated genes were influenced by rotarod training, respectively (Figure 4B, Table S4). Only 29 upregulated and 10 downregulated genes overlapped between the WT and *Tlr7*$^{-/y}$ groups (Figure 4B, Table S5). These data suggest that Tlr7 knockout alters gene expression caused by rotarod training.

We employed STRING to analyze the differentially expressed genes (DEG). In WT mice, "response to topologically incorrect protein", "ER" and "stress response" were three notable gene ontology (GO) terms for upregulated DEG (Figure 4C), suggesting that rotarod training induced a stress response even at molecular levels. For downregulated DEG in WT mice, GO terms were highly relevant to development, cell proliferation, response to endogenous stimulation, and transcriptional regulation (Figure 4D), consistent with the effect of rotarod training on altering neural differentiation and neurogenesis (Figures 3E and 3F). This outcome further indicates that rotarod training impairs responses to stimulation and transcriptional regulation and that it likely results in defective neurogenesis and differentiation in WT brains. For *Tlr7*$^{-/y}$ mice, STRING analysis did not reveal any notable GO terms, except that many upregulated DEG contained a signal peptide or a disulfide bond (Figures 4E and 4F). For the combined 39 overlapping DEG shared by WT and *Tlr7*$^{-/y}$ mice, no particular GO terms were apparent (Figure 4G).

Next, we used Ingenuity Pathway Analysis (IPA) to characterize the identified DEG. We found that the DEG of WT mice were associated with several protein networks, with three of them controlling behavior, nervous system development and function, and neurological disorders (Figure 5A), echoing the phenotype of WT mice that underwent the rotarod treatment. For *Tlr7*$^{-/y}$ mice, only one network was apparently relevant to behavioral features, i.e., that related to cell-to-cell signaling and neurological and psychological diseases (Figure 5A). Together, these analyses suggest that rotarod treatment elicits differential gene expression in WT and *Tlr7*$^{-/y}$ mice, but *Tlr7*$^{-/y}$ mice seem to be less sensitive to the impacts of rotarod training.

Overlapping DEG are relevant to anxiety

Since we found that rotarod training induces anxiety in both WT and *Tlr7*$^{-/y}$ mice, we expected that the overlapping DEG would have some relevance to anxiolytic behaviors. However, neither STRING nor IPA analyses presented an association of overlapping DEG with anxiety. Apart from *Il6*, we anticipated that more genes relevant to anxiety are regulated in both WT and *Tlr7*$^{-/y}$ mice. Therefore, we manually annotated the overlapping DEG by searching PubMed (https://www.ncbi.nlm.nih.gov). Of the 39 overlapping DEG, 26 (66%) of them have been associated with anxiety, depression or other mental disorders in patient studies and/or animal models (Figure 5B). Thus, together with IL-6, these 26 overlapping DEG appear to control expression of anxiety to rotarod training.

Tlr7 deletion diminishes the negative effect of rotarod training on expression of genes related to memory and neurogenesis

We then investigated how *Tlr7* deletion benefits spatial learning and memory in mice. We speculated that genes less sensitive or even resistant to rotarod treatment in *Tlr7*$^{-/y}$ mice would more likely be relevant to the better learning performance of the *Tlr7*$^{-/y}$ + RR group. We used heatmaps to compare gene expression among the four groups of mice. We observed very similar expression levels of the 39 overlapping DEG in the WT + RR and *Tlr7*$^{-/y}$ + RR groups (Figure 5C). For genes belonging to WT-specific GO, such as ER unfolded protein response, neuronal differentiation, cell death and behaviors, the WT + RR and *Tlr7*$^{-/y}$ + RR groups still presented the same expression tendency (either up- or down-regulation) (Figure 5C). Those genes were not present in the list of *Tlr7*$^{-/y}$ DEG because their expression was already reduced in the *Tlr7*$^{-/y}$–RR group. The effect of rotarod treatment was therefore diminished when we compared the *Tlr7*$^{-/y}$–RR and *Tlr7*$^{-/y}$ + RR groups. Nevertheless, this heatmap comparison allowed us to observe that expressions of some genes, such as *Tbx21*, *Frmd7* and others, were indeed less sensitive to rotarod training in *Tlr7*$^{-/y}$ mice (Figure 5C).

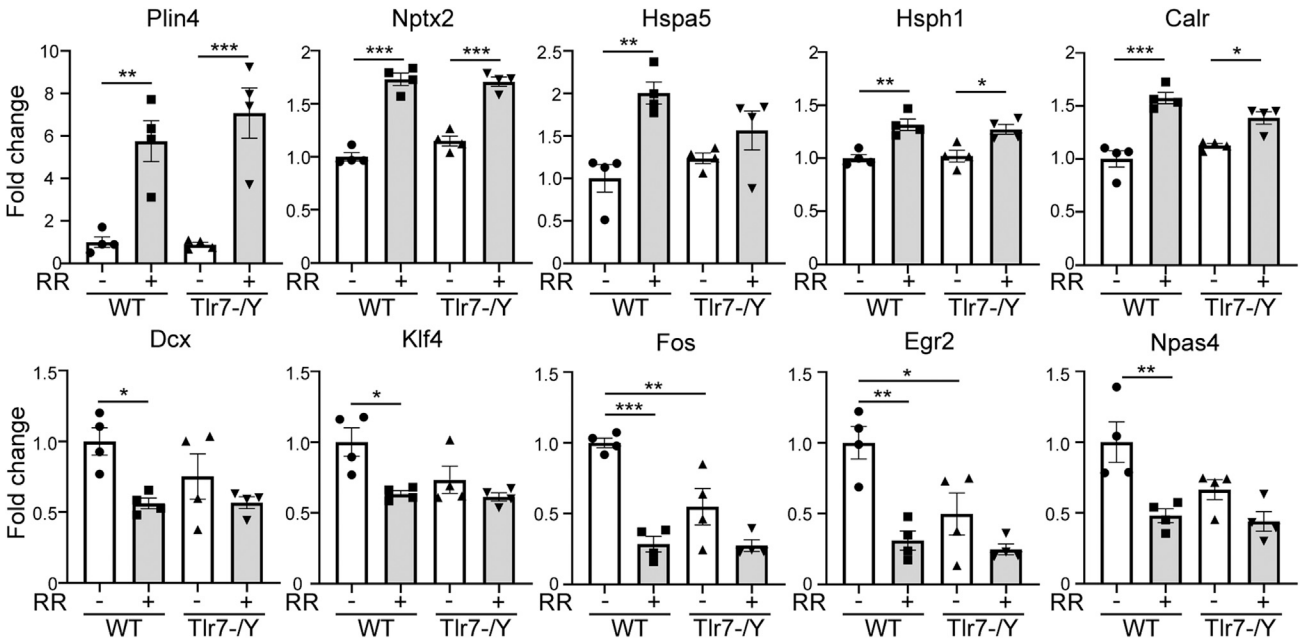

Figure 6. Quantitative RT-PCR verifies differential expression of DEGs identified from RNA-seq

A total of ten DEGs were selected from the heatmap shown in Figure 5C for quantitative RT-PCR. Data represent mean ± SEM. The results of individual animals are also shown. The sequences of primers and the numbers of Universal probes for PCR are available in Table S6. two-way ANOVA with Bonferroni's multiple comparisons test showed that rotarod treatment altered expression of all ten examined genes compared with mock control. The results of post-testing on significant differences are indicated. *, $p < 0.05$; **, $p < 0.01$; ***, $p < 0.001$. Sample size N = 4.

To verify the results of our RNA-seq analysis, we analyzed via quantitative RT-PCR the expression levels of a total of ten genes, including *Plin4*, *Nptx2*, *Hspa5*, *Hsph1*, *Calr*, *Dcx*, *Klf4*, *Fos*, *Egr2*, and *Npas4*. PLIN4, NPTX2, HSPA5, FOS, EGR2, and NPAS4 are all relevant to anxiety (Figure 5B). HSPA5, HSPH1 and CALR also participate in the ER unfolded protein response (Figure 5C). DCX and KLF4 are involved in neuronal differentiation (Figure 5C). It is also well known that FOS, EGR2, and NPAS4 contribute to neuronal activation. The results of quantitative RT-PCR were generally consistent with the results of RNA-seq (Figure 6), confirming the reliability of our RNA-seq analysis.

We further applied the same heatmap analysis to the total of 137 downregulated DEG in WT mice and found that 105 of them presented smaller changes in the *Tlr7*$^{-/y}$ + RR group relative to the WT + RR group, i.e., the ratio of normalized *Tlr7*$^{-/y}$ + RR expression to normalized WT + RR expression was greater than 1 (Figure 7A; Table S6). Based on STRING and Metascape analyses, these 105 rotarod-resistant genes were highly relevant to signal transduction, neurogenesis, neuron differentiation, development and transcription (Figures 7B and 7C). More specifically, thirteen of these rotarod-resistant genes have been found to play roles in learning and memory (Table S7, red font), ten are relevant to neurogenesis (Table S7, green font), and thirty-nine are involved in neuronal and/or brain functions (Table S7, brown font). These results indicate that *Tlr7* deletion exerts a protective effect to regulate the gene expression controlled by rotarod training. Altered expression of these rotarod-resistant genes in *Tlr7*$^{-/y}$ mice may regulate the activity of other DEG in the network (Figure 7B) to influence learning and memory of mice.

DISCUSSION

In the current report, we show that rotarod training, a regular test for motor coordination and balance, are actually able to induce anxiety and alter spatial learning/memory of mice via at least two different mechanisms. One is an IL-6-dependent pathway, which is involved in rotarod-induced anxiety. The other is via TLR7-regulated gene expression, which is critical for spatial learning/memory. Our study strengthens the role of neuronal innate immunity in controlling emotion and cognitive function and also unexpectedly reveals an impact of rotarod training on brain function. Since rotarod training influences anxiety and spatial learning/memory, caution should be taken when rotarod test and other behavioral assays are being arranged to analyze the same animals. These results also imply that exercise training might not always be

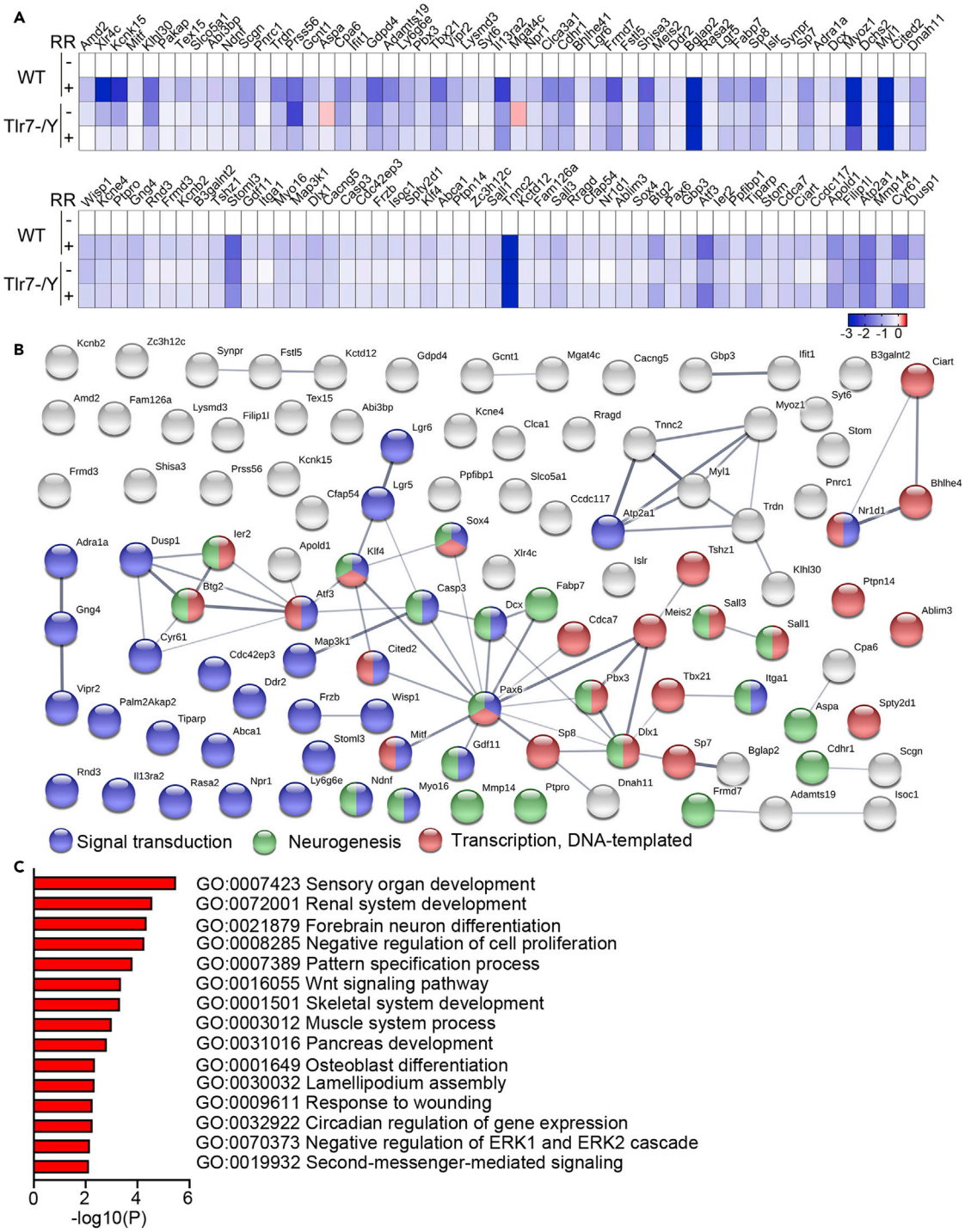

Figure 7. *Tlr7* deletion influences the expression of DEG regulated by rotarod training

(A) Heatmaps of downregulated DEG. The genes listed here have expression ratios of *Tlr7*$^{-/y}$ + RR to WT + RR greater than 1 (Table S3). Relative expression levels (log2) were normalized to WT–RR. The color-coded bar represents the *Z* score.

(B) STRING analysis of the protein networks of selected genes (the same gene set in A). Node color represents an association with the different networks indicated at the bottom.

(C) Gene ontology analysis of selected genes assessed using Metascape.

positive for cognitive and emotional responses. Stressful duress in exercise training may result in negative effects. Although it is unclear if stressful exercise training also results in negative effects in human, we advocate carefully designing training programs to avoid potential negative effects.

Although our study suggests that rotarod-dependent regulation is highly relevant to IL-6 and TLR7, two important innate immune regulators, neither astrocytes nor microglial cells were activated by rotarod training. Thus, the effect of IL-6 and TLR7 may primarily act on neurons. Indeed, previous findings have indicated that neurons express various cytokines, including IL-6 (Hung et al., 2018a; Liu et al., 2013; Wu et al., 2016) and different TLRs, such as TLR3, TLR7, and TLR8 (Chen et al., 2017; Hung et al., 2018b; Liu et al., 2015). It is know that IL-6 regulates neuronal morphology (Liu et al., 2013) and anxious behaviors (Lazaridou et al., 2018; O'Donovan et al., 2010). TLR3, TLR7 and TLR8 all cell-autonomously fine-tune neuronal morphology, including axonal and dendritic growth and/or dendritic spine formation (Chen et al., 2017; Hung et al., 2018b; Liu et al., 2013). Rotarod training likely controls expression and/or activity of IL-6 and TLR7, thereby influencing anxiety and spatial learning/memory of mice.

Note, the impact of rotarod training and TLR7 on different spatial memory tests varied. For WT mice, rotarod pretraining did not affect the spatial memory in contextual fear conditioning and Barnes maze assays, but it did slow down the learning process in Barnes maze. However, upon *Tlr7* knockout, rotarod pretreatment enhanced contextual fear memory and facilitated spatial learning in Barnes maze. Thus, Tlr7 knockout appears to neutralize or even reverse the negative effect of rotarod training on spatial learning/memory. Our transcriptomic analyses further indicate that the beneficial effect of rotarod training on learning and memory in $Tlr7^{-/y}$ mice likely arises through altered expression of genes controlling neurogenesis and mouse behaviors.

In our experiment, the mice performed rotarod pretraining at least two weeks before undertaking other behavioral assays. Thus, the effect of rotarod training on anxiety and spatial learning/memory is long-lasting. Many genes involved in the ER-related unfolding protein response were upregulated 3 hr after rotarod training, echoing our observation that rotarod exercise does indeed induce a stress response, at least in the cortex and hippocampus. Based on our transcriptomic profiling, we noticed that several transcriptional regulators were impacted by rotarod training, suggesting that altered regulation of gene expression is likely involved in the long-lasting effect of forced rotarod exercise. Since our data indicate an involvement of TLR7 and given that our previous study demonstrated that TLR7 activation in neurons can evoke the MYD88-dependent pathway to induce C-FOS expression (Liu et al., 2013), TLR7 likely contributes to the transcriptional regulation induced by rotarod exercise. Moreover, TLR7 can recognize endogenous miRNA (Lehmann et al., 2012; Liu et al., 2015). Therefore, since miRNA can be transported via exosomes to activate TLR7 (Lehmann et al., 2012; Liu et al., 2015), it would be very intriguing to explore if miRNAs/exosomes represent critical mediators of how forced rotarod exercise controls TLR7 activation and consequently influence transcriptional and behavioral changes.

For typical forced exercise, treadmill is a popular model for rodents (Contarteze et al., 2008; Svensson et al., 2016). It is a very stressful treatment that induces global inflammation in both brain and peripheral tissues (Cook et al., 2013; Nambot et al., 2020; Svensson et al., 2016). In this report, we found that rotarod testing also influence *Il-6* expression in cortices and hippocampi. The rotarod test is a much milder task compared to treadmill, as we found that it did not trigger cytokine expression in mouse spleen. However, the duress of being placed on the moving rod is sufficient to increase *Il6* mRNA levels in the cortex and hippocampus and it has a long-term impact on mouse behaviors. Thus, a rotarod test can serve as a relatively specific model to investigate the effect of forced exercise-induced stress on brains.

Limitations of the study

First, although we have demonstrated the involvement of IL-6 and TLR7 in rotarod-regulated anxiety and spatial learning/memory, we are still unsure how rotarod training modulates gene expression, including of *Il-6*. The signal pathway operating downstream of rotarod training remains unclear. Second, we have focused on the effect of rotarod training on the cortex and hippocampus because these two brain regions are highly relevant to anxiety and spatial learning/memory. Since it is unclear if any specific region accounts for the effect of rotarod training, we pooled cortex and hippocampus together for analysis. We have identified and validated several DEGs from the mixed hippocampus and cortex samples in this report. It would be illuminating to further explore more specific brain regions, such as dorsal or ventral hippocampi and somatosensory, cingulate or motor cortices, and also to investigate the role of other brain regions. Third, we found that rotarod training at 5 weeks old had a stronger effect on anxiety and locomotion compared to training at 10 weeks old. Thus, rotarod training at 5 weeks could

likely serve as a model to investigate how early life experiences influence emotion and cognitive activity in adults, warranting further investigation. Finally, we used male mice in the current report. We do not know whether female mice are also sensitive or even more susceptible to rotarod training. Given that the prevalence of anxiety disorders is much higher for women than men (https://www.texashealth.org/Health-and-Wellness/Behavioral-Health/How-Anxiety-Affects-Men-and-Women-Differently), it would be intriguing to compare the responses of female and male mice to rotarod training. Thus, sex-biased effects need to be considered in future studies.

Resource availability

Lead contact

Further information and requests for resources and reagents should be directed to and will be fulfilled by the lead contact, Yi-Ping Hsueh (yph@gate.sinica.edu.tw).

Materials availability

All unique/stable reagents generated in this study are available from the lead contact with a completed Materials Transfer Agreement of Academia Sinica.

Data and code availability

The accession number for the RNA-seq reported in this paper is NCBI BioProject: PRJNA702827.

METHODS

All methods can be found in the accompanying transparent methods supplemental file.

SUPPLEMENTAL INFORMATION

Supplemental information can be found online at https://doi.org/10.1016/j.isci.2021.102384.

ACKNOWLEDGMENTS

We thank the Genomics Core, the Bioinformatics Core and the Animal Facility of the Institute of Molecular Biology, Academia Sinica, for excellent technical assistance, and Dr. John O'Brien for English editing. This work was supported by grants from Academia Sinica (AS-IA-106-L04) and the Ministry of Science and Technology (MOST 108-2311-B-001-008-MY3) to Y.-P. Hsueh.

AUTHOR CONTRIBUTIONS

Conceptualization, Y.-F.H., and Y.-P.H.; methodology and investigation, Y.-F.H.; writing, Y.-F.H., and Y.-P.H.; funding acquisition, Y.- P.H.; supervision and project administration, Y.-P.H.

DECLARATION OF INTERESTS

The authors declare no competing interests.

Received: September 8, 2020
Revised: February 20, 2021
Accepted: March 30, 2021
Published: April 23, 2021

REFERENCES

Akira, S., and Sato, S. (2003). Toll-like receptors and their signaling mechanisms. Scand. J. Infect. Dis. *35*, 555–562.

Bettio, L., Thacker, J.S., Hutton, C., and Christie, B.R. (2019). Modulation of synaptic plasticity by exercise. Int. Rev. Neurobiol. *147*, 295–322.

Bilbo, S.D., Block, C.L., Bolton, J.L., Hanamsagar, R., and Tran, P.K. (2018). Beyond infection - Maternal immune activation by environmental factors, microglial development, and relevance for autism spectrum disorders. Exp. Neurol. *299*, 241–251.

Burgueño, J.F., and Abreu, M.T. (2020). Epithelial Toll-like receptors and their role in gut homeostasis and disease. Nat. Rev. Gastroenterol. Hepatol. *17*, 263–278.

Caputi, V., and Giron, M.C. (2018). Microbiome-gut-brain Axis and toll-like receptors in Parkinson's disease. Int. J. Mol. Sci. *19*, 1689.

Chen, C.Y., Liu, H.Y., and Hsueh, Y.P. (2017). TLR3 downregulates expression of schizophrenia gene Disc1 via MYD88 to control neuronal morphology. EMBO Rep. *18*, 169–183.

Chen, C.Y., Shih, Y.C., Hung, Y.F., and Hsueh, Y.P. (2019). Beyond defense: regulation of neuronal morphogenesis and brain functions via Toll-like receptors. J. Biomed. Sci. *26*, 90.

Contarteze, R.V., Manchado Fde, B., Gobatto, C.A., and De Mello, M.A. (2008). Stress

biomarkers in rats submitted to swimming and treadmill running exercises. Comp. Biochem. Physiol. A. Mol. Integr. Physiol. *151*, 415–422.

Cook, M.D., Martin, S.A., Williams, C., Whitlock, K., Wallig, M.A., Pence, B.D., and Woods, J.A. (2013). Forced treadmill exercise training exacerbates inflammation and causes mortality while voluntary wheel training is protective in a mouse model of colitis. Brain Behav. Immun. *33*, 46–56.

Cooper, C., Moon, H.Y., and van Praag, H. (2018). On the run for hippocampal plasticity. Cold Spring Harb. Perspect. Med. *8*, a029736.

De Miguel, Z., Haditsch, U., Palmer, T.D., Azpiroz, A., and Sapolsky, R.M. (2019). Adult-generated neurons born during chronic social stress are uniquely adapted to respond to subsequent chronic social stress. Mol. Psychiatry *24*, 1178–1188.

de Quervain, D., Schwabe, L., and Roozendaal, B. (2017). Stress, glucocorticoids and memory: implications for treating fear-related disorders. Nat. Rev. Neurosci. *18*, 7–19.

Delezie, J., and Handschin, C. (2018). Endocrine crosstalk between skeletal muscle and the brain. Front. Neurol. *9*, 698.

Duman, R.S., and Li, N. (2012). A neurotrophic hypothesis of depression: role of synaptogenesis in the actions of NMDA receptor antagonists. Philos. Trans. R. Soc. Lond. B Biol. Sci. *367*, 2475–2484.

Gold, P.W., Licinio, J., and Pavlatou, M.G. (2013). Pathological parainflammation and endoplasmic reticulum stress in depression: potential translational targets through the CNS insulin, klotho and PPAR-γ systems. Mol. Psychiatry *18*, 154–165.

Gold, P.W., Machado-Vieira, R., and Pavlatou, M.G. (2015). Clinical and biochemical manifestations of depression: relation to the neurobiology of stress. Neural Plast. *2015*, 581976.

Gusel'nikova, V.V., and Korzhevskiy, D.E. (2015). NeuN as a neuronal nuclear antigen and neuron differentiation marker. Acta Nat. *7*, 42–47.

Hamilton, G.F., and Rhodes, J.S. (2015). Exercise regulation of cognitive function and neuroplasticity in the healthy and diseased brain. Prog. Mol. Biol. Transl Sci. *135*, 381–406.

Hotamisligil, G.S. (2010). Endoplasmic reticulum stress and the inflammatory basis of metabolic disease. Cell *140*, 900–917.

Hung, Y.F., Chen, C.Y., Li, W.C., Wang, T.F., and Hsueh, Y.P. (2018a). Tlr7 deletion alters expression profiles of genes related to neural function and regulates mouse behaviors and contextual memory. Brain Behav. Immun. *72*, 101–113.

Hung, Y.F., Chen, C.Y., Shih, Y.C., Liu, H.Y., Huang, C.M., and Hsueh, Y.P. (2018b). Endosomal TLR3, TLR7, and TLR8 control neuronal morphology through different transcriptional programs. J. Cell Biol. *217*, 2727–2742.

Khandaker, G.M., Cousins, L., Deakin, J., Lennox, B.R., Yolken, R., and Jones, P.B. (2015). Inflammation and immunity in schizophrenia: implications for pathophysiology and treatment. Lancet Psychiatry *2*, 258–270.

Knuesel, I., Chicha, L., Britschgi, M., Schobel, S.A., Bodmer, M., Hellings, J.A., Toovey, S., and Prinssen, E.P. (2014). Maternal immune activation and abnormal brain development across CNS disorders. Nat. Rev. Neurol. *10*, 643–660.

Kumar, H., Kawai, T., and Akira, S. (2009). Toll-like receptors and innate immunity. Biochem. Biophys. Res. Commun. *388*, 621–625.

Lazaridou, A., Martel, M.O., Cahalan, C.M., Cornelius, M.C., Franceschelli, O., Campbell, C.M., Haythornthwaite, J.A., Smith, M., Riley, J., and Edwards, R.R. (2018). The impact of anxiety and catastrophizing on interleukin-6 responses to acute painful stress. J. Pain Res. *11*, 637–647.

Lehmann, S.M., Kruger, C., Park, B., Derkow, K., Rosenberger, K., Baumgart, J., Trimbuch, T., Eom, G., Hinz, M., Kaul, D., et al. (2012). An unconventional role for miRNA: let-7 activates Toll-like receptor 7 and causes neurodegeneration. Nat. Neurosci. *15*, 827–835.

Lin, C., Zhao, S., Zhu, Y., Fan, Z., Wang, J., Zhang, B., and Chen, Y. (2019). Microbiota-gut-brain axis and toll-like receptors in Alzheimer's disease. Comput. Struct. Biotechnol. J. *17*, 1309–1317.

Liu, H.Y., Chen, C.Y., and Hsueh, Y.P. (2014). Innate immune responses regulate morphogenesis and degeneration: roles of Toll-like receptors and Sarm1 in neurons. Neurosci. Bull. *30*, 645–654.

Liu, H.Y., Hong, Y.F., Huang, C.M., Chen, C.Y., Huang, T.N., and Hsueh, Y.P. (2013). TLR7 negatively regulates dendrite outgrowth through the Myd88-c-Fos-IL-6 pathway. J. Neurosci. *33*, 11479–11493.

Liu, H.Y., Huang, C.M., Hung, Y.F., and Hsueh, Y.P. (2015). The microRNAs Let7c and miR21 are recognized by neuronal Toll-like receptor 7 to restrict dendritic growth of neurons. Exp. Neurol. *269*, 202–212.

Nambot, S., Faivre, L., Mirzaa, G., Thevenon, J., Bruel, A.L., Mosca-Boidron, A.L., Masurel-Paulet, A., Goldenberg, A., Le Meur, N., Charollais, A., et al. (2020). De novo TBR1 variants cause a neurocognitive phenotype with ID and autistic traits: report of 25 new individuals and review of the literature. Eur. J. Hum. Genet. *28*, 770–782.

O'Donovan, A., Hughes, B.M., Slavich, G.M., Lynch, L., Cronin, M.T., O'Farrelly, C., and Malone, K.M. (2010). Clinical anxiety, cortisol and interleukin-6: evidence for specificity in emotion-biology relationships. Brain Behav. Immun. *24*, 1074–1077.

Pedersen, B.K. (2019). Physical activity and muscle-brain crosstalk. Nat. Rev. Endocrinol. *15*, 383–392.

Pittenger, C., and Duman, R.S. (2008). Stress, depression, and neuroplasticity: a convergence of mechanisms. Neuropsychopharmacology *33*, 88–109.

Rendeiro, C., and Rhodes, J.S. (2018). A new perspective of the hippocampus in the origin of exercise-brain interactions. Brain Struct. Funct. *223*, 2527–2545.

Ryan, S.M., and Nolan, Y.M. (2016). Neuroinflammation negatively affects adult hippocampal neurogenesis and cognition: can exercise compensate? Neurosci. Biobehav Rev. *61*, 121–131.

Sommer, F., and Bäckhed, F. (2013). The gut microbiota–masters of host development and physiology. Nat. Rev. Microbiol. *11*, 227–238.

Spiljar, M., Merkler, D., and Trajkovski, M. (2017). The immune system bridges the gut microbiota with systemic energy homeostasis: focus on tlrs, mucosal barrier, and SCFAs. Front. Immunol. *8*, 1353.

Svensson, M., Rosvall, P., Boza-Serrano, A., Andersson, E., Lexell, J., and Deierborg, T. (2016). Forced treadmill exercise can induce stress and increase neuronal damage in a mouse model of global cerebral ischemia. Neurobiol. Stress *5*, 8–18.

Voss, M.W., Soto, C., Yoo, S., Sodoma, M., Vivar, C., and van Praag, H. (2019). Exercise and hippocampal memory systems. Trends Cogn. Sci. *23*, 318–333.

Wu, P.J., Liu, H.Y., Huang, T.N., and Hsueh, Y.P. (2016). AIM 2 inflammasomes regulate neuronal morphology and influence anxiety and memory in mice. Sci. Rep. *6*, 32405.

Yiu, J.H., Dorweiler, B., and Woo, C.W. (2017). Interaction between gut microbiota and toll-like receptor: from immunity to metabolism. J. Mol. Med. (Berl) *95*, 13–20.

iScience, Volume *24*

Supplemental information

TLR7 and IL-6 differentially regulate the effects of rotarod exercise on the transcriptomic profile and neurogenesis to influence anxiety and memory

Yun-Fen Hung and Yi-Ping Hsueh

SUPPLEMENTAL FIGURES AND FIGURE LEGENDS

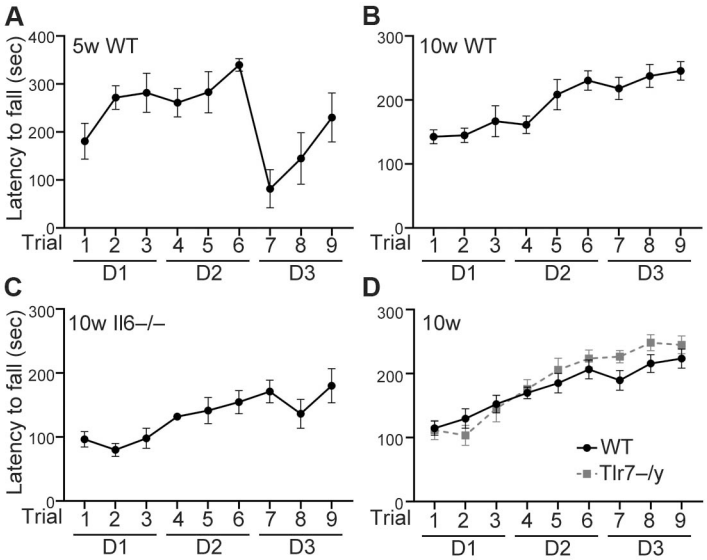

Supplemental Figure S1. The performance of wild-type, *Il6*$^{-/-}$ and *Tlr7*$^{-/y}$ mice on rotarod (related to Figures 1, 2 and 3).

Wild-type (WT) 5-week-old (**A**) and 10-week-old (**B**) mice, 10-week-old *Il6*$^{-/-}$ mice (**C**), and 10-week-old WT and *Tlr7*$^{-/y}$ mice (**D**) were subjected to accelerating rotarod test on three consecutive days. Latency to fall, i.e. the time period to stay on the rotarod, is shown. The curve in (**A**) is quite different from the curves in (**B**)-(**D**) because 5-week-old mice tended to jump away from the rotarod at Day 3. In (**D**), littermates were used to compare the effect of *Tlr7* knockout on rotarod. Similar to a previous report (Hung et al., 2018a), *Tlr7*$^{-/y}$ mice performed comparably to WT littermates in rotarod test. In conclusion, all tested mice at the age of 10 weeks can learn to stay on the rotarod and display better performance at Day 3 (D3). Data represent mean +/– SEM. Sample sizes have been shown in the legends of Figures 1, 2 and 3.

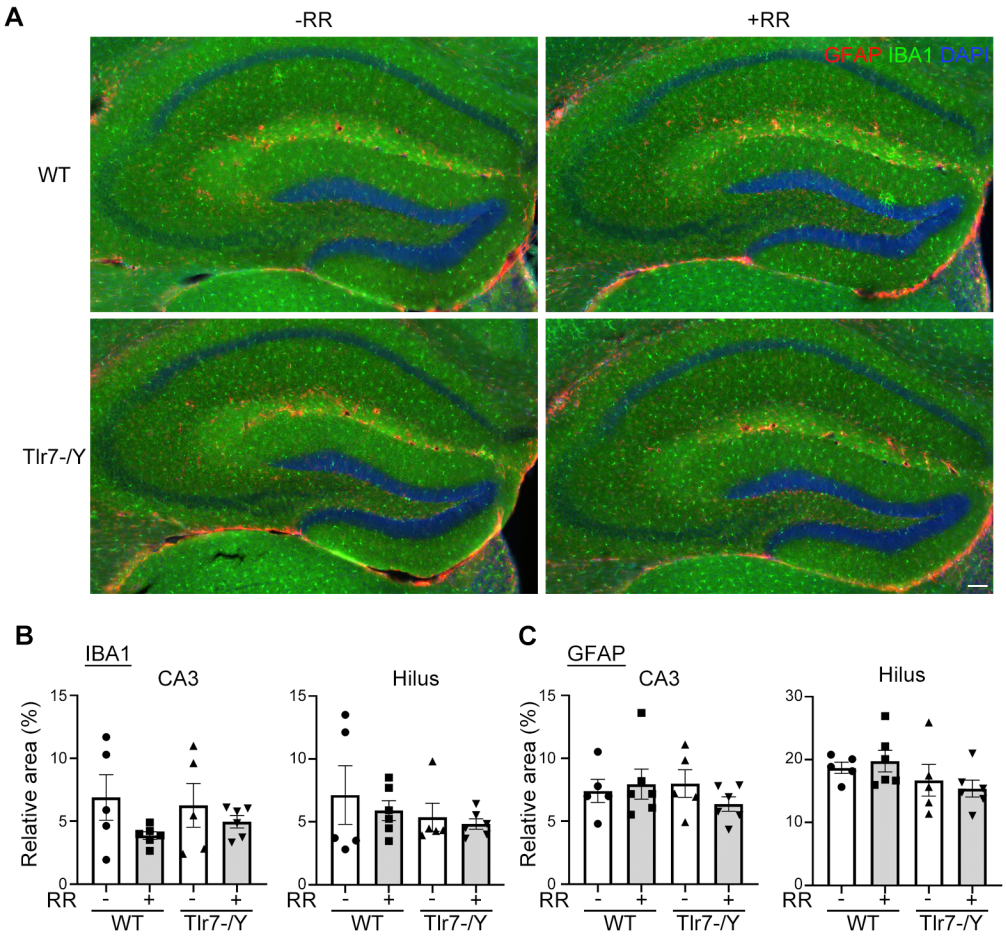

Supplemental Figure S2. Rotarod training does not alter the population of glial cells in either WT or *Tlr7*$^{-/y}$ mice (related to Figure 2).

A Representative images of GFAP (red) and IBA1 (green) dual immunostaining of hippocampus. Both WT and *Tlr7*$^{-/y}$ mice were subjected to rotarod training or mock control. **B-C** Quantification of relative area of IBA1 and GFAP immunoreactivities in CA3 and hilar regions. Data represent mean +/– SEM and the results of individual samples are shown. Two-way ANOVA test (B-C). Scale bar: 100 μm.

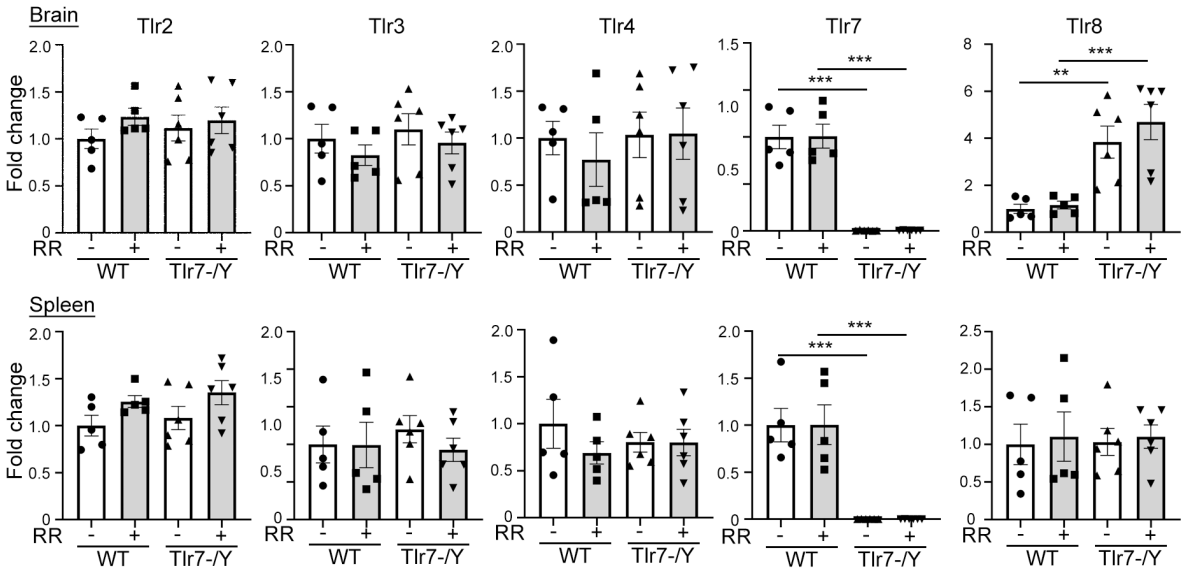

Supplemental Figure S3 Rotarod training does not change the expression of *Toll-like receptor* (*Tlr*) genes in mouse brain or spleen (related to Figure 2).

Quantitative PCR was performed to measure the expression levels of *Tlr2*, *Tlr3*, *Tlr4*, *Tlr7* and *Tlr8* in the brain and spleen of mice after undergoing rotarod training at 10 weeks of age. The results were normalized with internal control *Gapdh*. Rotarod training exerts no obvious change in expression of *Tlr* genes in brain or spleen of either WT or *Tlr7*$^{-/y}$ mice (n=5 for WT, n=6 for *Tlr7*$^{-/y}$). Data represent mean +/– SEM and the results of individual samples are shown. Two-way ANOVA with Bonferroni's multiple comparisons test. **, $P < 0.01$; *** $P < 0.001$.

SUPPLEMENTAL TABLES

Supplemental Table S1. Summary of animals used in this report (related to all Figures).

Supplemental Table S2. Q-PCR primers and UPL probes (related to Figures 2 and 6).

Supplemental Table S3. Key resource table (related to all Figures).

Supplemental Table S4. Quantitative analysis of differentially expressed genes influenced by rotarod training in WT and *Tlr7*$^{-/Y}$ mice (related to Figure 4, an Excel table)

Supplemental Table S5. List of differentially expressed genes in WT and *Tlr7*$^{-/y}$ mice with or without rotarod training (related to Figure 4).

Supplemental Table S6. Downregulated genes in WT mice that are less sensitive to rotarod training in *Tlr7*$^{-/Y}$ mice (related to Figure 7).

Supplemental Table S7. Selected genes from Supplemental Table S6 and their representative references relevant to physiological functions (related to Figure 7).

Supplemental Table S1. Summary of animals used in this report (related to all Figures).

Animal group number	Type of analysis	Rotarod treatment	Mouse line	Figures
I	Behavior	yes (5w)	WT	1B-1D
II	Behavior	no	WT	1B-1D
III	Behavior	yes (10w)	WT	1E-1G
IV	Behavior	no	WT	1E-1G
V	RNA collection	yes and no (10w)	WT, *Tlr7-/Y*	2A, 4, 5, 6, 7, S3
VI	Behavior	yes and no (10w)	*Il6–/–*	2B
VII	IBA1/GFAP staining	yes and no (10w)	*Il6–/–*	2C
VIII	Behavior	yes and no (10w)	WT, *Tlr7-/Y*	3C
IX	Behavior	yes and no (10w)	WT, *Tlr7-/Y*	3B, 3D
X	BrdU labeling	yes and no (10w)	WT, *Tlr7-/Y*	3E, 3F
XI	IBA1/GFAP staining	yes and no (10w)	WT, *Tlr7-/Y*	S2

Supplementary Table S2. Q-PCR primers and UPL probes (related to Figures 2 and 6).

Gene	Quantitative RT-PCR primer pairs	Probe
Il6	F: GCTACCAAACTGGATATAATCAGGA	#6
	R: CCAGGTAGCTATGGTACTCCAGAA	
Il1b	F: AGTTGACGGACCCCAAAAG	#38
	R: AGCTGGATGCTCTCATCAGG	
Tnfa	F: TTGTCTTAATAACGCTGATTTGGT	#64
	R: GGGAGCAGAGGTTCAGTGAT	
Ifnb	F: CACAGCCCTCTCCATCAACTA	#78
	R: CATTTCCGAATGTTCGTCCT	
Ccl5	F: TGCAGAGGACTCTGAGACAGC	#110
	R: GAGTGGTGTCCGAGCCATA	
Tlr2	F: GGGGCTTCACTTCTCTGCTT	#50
	R: AGCATCCTCTGAGATTTGACG	
Tlr3	F: GATACAGGGATTGCACCCATA	#26
	R: TCCCCCAAAGGAGTACATTAGA	
Tlr4	F: GGACTCTGATCATGGCACTG	#2
	R: CTGATCCATGCATTGGTAGGT	
Tlr7	F: TGATCCTGGCCTATCTCTGAC	#25
	R: CGTGTCCACATCGAAAACAC	
Tlr8	F: CAAACGTTTTACCTTCCTTTGTCT	#56
	R: ATGGAAGATGGCACTGGTTC	
Gapdh	F: AATGTGTCCGTCGTGGATCT	#80
	R: CCCAGCTCTCCCCATACATA	
Plin4	F: GCTGGAGTCAGTTACCGTCAA	#1
	R: CGCCTCCTTTTCCTCTCAT	
Nptx2	F: TCAAGGACCGCTTGGAGA	#78
	R: GCCCAGCGTTAGACACATTT	
Hspa5	F: CTGAGGCGTATTTGGGAAAG	#105
	R: TCATGACATTCAGTCCAGCAA	
Hsph1	F: AACCCCAGATGCTGACAAA	#75

	R: CCACCTTTATTTTAGGTTTCTTGG	
Calr	F: TGAAGCTGTTTCCGAGTGGT	#93
	R: GATGACATGAACCTTCTTGGTG	
Dcx	F: AGCTGACTCAGGTAACGACCA	#11
	R: GCTTTGACTTAGGTGTTGAGAGC	
Klf4	F: CGGGAAGGGAGAAGACACT	#62
	R: GAGTTCCTCACGCCAACG	
Fos	F: GGGACAGCCTTTCCTACTACC	#67
	R: AGATCTGCGCAAAAGTCCTG	
Egr2	F: CTACCCGGTGGAAGACCTC	#60
	R: AATGTTGATCATGCCATCTCC	
Npas4	F: AGGGTTTGCTGATGAGTTGC	#21
	R: TTCCCCTCCACTTCCATCTT	
Hprt	F: CCTCCTCAGACCGCTTTTT	#95
	R: AACCTGGTTCATCATCGCTAA	

Supplemental Table S3. Key resource table (related to all Figures).

REAGENT or RESOURCE	SOURCE	IDENTIFIER
Antibodies		
Rabbit anti-IBA1	FUJIFILM Wako Pure Chemical Corporation	Cat# 019-19741, RRID:AB_839504
Mouse monoclonal anti-GFAP (clone GA5)	Millipore	Cat# MAB3402, RRID:AB_94844
Rat monoclonal anti-BrdU [BU1/75 (ICR1)]	Abcam	Cat# ab6326, RRID:AB_305426
Goat polyclonal anti-DCX (C-18)	Santa Cruz Biotechnology	Cat# sc-8066, RRID:AB_2088494
Mouse monoclonal anti-NeuN	Millipore	Cat# MAB377, RRID:AB_2298772
Experimental Models: Organisms/Strains		
Mouse: B6.129S1-Tlr7tm1Flv/J	The Jackson Laboratory	RRID:IMSR_JAX:008380
Mouse:B6;129S2-Il6tm1Kopf/J	The Jackson Laboratory	RRID:IMSR_JAX:002254
Mouse: B6	Taiwan National Laboratory Animal Center	N/A
Chemicals, Peptides, and Recombinant Proteins		
5-Bromo-2′-deoxyuridine	Sigma-Aldrich	B5002;CAS: 59-14-3
Oligonucleotides		
Primers for QPCR, see Table S5	This paper	N/A
Critical Commercial Assays		
Truseq Stranded mRNA kit	Illumina	1.48v
Transcriptor First Strand cDNA Synthesis Kit	Roche	N/A
LightCycler® 480 Probes Master	Roche	N/A
Universal Probe Library probes	Roche	N/A
Software and Algorithms		
ImageJ	https://imagej.nih.gov/ij/	1.48v
Smart Video Tracking System	Panlab, Barcelona, Spain	N/A
FreezeScan	CleverSys Inc., Reston, VA, USA	2.0
LightCycler480	Roche	1.5.0

UPL Assay Design Center Web Service	https://lifescience.roche.com/en_tw/brands/universal-probe-library.html#assay-design-center	N/A
CLC Genomics Workbench	https://www.qiagenbioinformatics.com/	v.10.1.1
Metascape	http://metascape.org/gp/index.html	N/A
IPA	QIAGEN	N/A
STRING	https://string-db.org/	N/A
Zen Blue	Zeiss	3.1
LSM700	Zeiss	N/A
Prism	GraphPad	8.0
Deposited Data		
Raw data	This paper	NCBI BioProject ID PRJNA702827

TRANSPARENT METHODS

EXPERIMENTAL MODEL AND SUBJECT DETAILS

Wild type C57BL/6 male mice were purchased from the Taiwan National Laboratory Animal Center for behavioral analyses. *Tlr7*$^{-/y}$ mice (Lund et al., 2004) and *Il6*$^{-/-}$ mice (Kopf et al., 1994) in a C57BL/6 genetic background were originally imported from the Jackson Laboratory and bred and maintained in the animal facility of the Institute of Molecular Biology (IMB), Academia Sinica, with a 14 h light/10 h dark cycle and controlled temperature (20-23 °C) and humidity (48-55%) under pathogen-free conditions. For behavioral assays, mice were transferred to the behavioral room of IMB with a 12 h light/12 h dark cycle for at least 1 week before experiments. Only male mice were used for behavioral analyses. The mice were group-housed with their littermates and each cage contained 3 to 5 mice. All animal experiments were performed with the approval of the Academia Sinica Institutional Animal Care and Utilization Committee (Protocol No. 13-02-520) and in strict accordance with its guidelines and those of the Council of Agriculture Guidebook for the Care and Use of Laboratory Animals.

To investigate the effect of forced rotarod exercise on mouse behaviors, we subjected mice to an accelerating rotarod test for three consecutive days before they underwent various behavioral assays at various later timeframes. The temperature (20-23 °C) and humidity (48-55%) of the behavioral room were controlled and it was equipped with a light intensity of 240 lumen/m2 (lux). All behavioral experiments were assayed during daytime from 10 am ~ 5 pm. All behavioral assays used in this manuscript were based on previous publications (Hsu et al., 2020; Hu et al., 2020; Huang et al., 2019; Huang et al., 2021; Hung et al., 2018a; Lin and Hsueh, 2014; Shih et al., 2020a; Shih et al., 2020b; Wu et al., 2017). The details are described below.

METHOD DETAILS

Behavioral tasks:

Accelerating rotarod

To ensure that mice could stay stably on the drum, mice were placed on the resting drum (3 cm in diameter) of a rotarod apparatus (RT-01, SINGA, Diagnostic & Research Instruments Co. Taoyuan, Taiwan) for at least 1 min. The speed of the rotarod was accelerated from 0 to 40 rpm over a 5-min period for mice at 10 weeks of age or a 6-min period for mice at 5 weeks of age. The mice were subjected to three trials per day, with 10-15 min intervals

between trails, for 3 consecutive days. Latency to fall in each trial was recorded. The apparatus was cleaned with 70% ethanol and air-dried between usages by different animals. Mock control mice were either placed on a non-moving rotarod for 5 min or without treatment. Since there was no difference between these two kinds of controls, it is not specified in this report.

Open field

The apparatus of open field was a transparent plastic box (40×40×32.5 cm). Before the assay, the experimental mouse was placed in a new cage for 10 min before being transferred to the center region of the transparent box. Their movements were recorded for 10 min by videotaping from above. The grooming, rearing, urine and stool number was counted manually. Rearing was defined as both forelimbs leaving the ground. The total moving distance, speed and the time spent in the four corners (10×10 cm for each corner) and the center (20×20 cm) were quantified with the Smart Video Tracking System (Panlab, Barcelona, Spain). The apparatus was cleaned with 70% ethanol and air-dried before being used for another mouse.

Elevated plus maze

The maze comprised two open-sided arms (30×5 cm) and two arms (30×5 cm) enclosed by a 14-cm-high wall. The central platform was a square of 5 cm and the entire apparatus was raised 45.5 cm above ground level. An individual mouse was placed into the central area facing one of the open-sided arms and allowed to freely explore the maze for 10 min. Mouse movements were recorded from above using a videocamera. The time spent in different areas was analyzed using the Smart Video Tracking System (Panlab, Barcelona, Spain). The maze was cleaned with 70% ethanol and air-dried before assaying another mouse.

Barnes maze

The maze was a white circular platform (100 cm in diameter) with 40 holes (5 cm in diameter) cut into the periphery. An escape box (black plastic box, 8×20×5 cm) was attached magnetically under one of the holes (target hole). At day 0, an individual mouse was put into a cylindrical start chamber in the middle of the maze and, upon removing the start chamber, it was guided to enter the target hole. Once the mouse had entered the target hole, the hole was covered and the mouse remained there for 2 min. In the training phase, mice were allowed to freely explore the maze individually until they had entered the target hole within 180 sec. If a

mouse had not escaped through the target hole within 180 sec, it was guided there by the experimenter and its escape latency was recorded as 180 sec. Experimental mice underwent four trials per day, with 15 min intervals between trials, for 4 consecutive days. Escape latency was measured as the time taken to enter the target hole from removing the start chamber. In a probe assay (day 5 and day 12), the target hole was covered and experimental mice were allowed to freely explore the maze for 90 sec. In all cases, mouse movements were recorded by videotaping from above using a wide-angle lens. The time taken to reach the target hole was quantified using the Smart Video Tracking System (Panlab, Barcelona, Spain). The apparatus was cleaned with 70% ethanol and air-dried between usages by different animals.

Fear conditioning

A fear conditioning chamber (Med Associates Inc., Fairfax, VT, USA) supported with the FreezeScan 2.0 analytical system (CleverSys Inc., Reston, VA, USA) was used to analyze the fear memory of mice. At day 1, an experimental mouse was habituated in Box A (a transparent plastic box) for 12 min. The freezing percentage during these 12 min was averaged to represent the "basal" freezing response. At day 2, an individual mouse was placed into Box B (a transparent colored box with slips of colored paper on the walls) containing scent of 1% acetic acid. After 4 min, three paired stimulations comprising a tone (2 kHz; 80 dB; 20 s) followed by an electronic foot shock (0.6 mA; 2 s) were applied with one min intervals. The freezing percentage within 1 minute directly after the third foot shock was used to represent the response "after stimulation (AS)", indicating the immediate response that is relevant to pain sensation of mice to foot shock. At day 3, mice were again placed in Box B for 12 min without experiencing tone or foot shock stimulations. The freezing responses from 3-6 min after entering Box B were averaged to indicate contextual fear memory. At day 4, the experimental mouse was placed into Box A for 4 min and then received twenty tones (2 kHz; 80 dB; 20 s) separated by 5-s intervals. The freezing responses of mice were averaged from the first six tones to indicate cued fear memory.

Quantitative RT-PCR (Q-PCR).

Three hours after rotarod training, mouse cortices and hippocampi were collected by removing the olfactory bulb and entire subcortical regions from whole brains. Cortical and hippocampal tissues were immediately lyzed in Trizol reagent by dounce homogenization and then stored at -80 °C until RNA extraction according to the manufacturer's instructions

(Invitrogen), followed by DNase I (New England BioLabs) digestion for 30 min at 37 °C to remove contaminating DNA. RNA isolated from mouse brain was then used for cDNA synthesis by the Transcriptor First Strand cDNA Synthesis Kit (Roche) with an oligo(dT)18 primer. A real-time PCR assay was performed using the LightCycler480 (Roche) and Universal Probe Library probes (UPL, Roche) system. The primers and their paired probes (see **Supplemental Table S2**) were designed using the Assay Design Center Web Service (Roche). The PCR thermal profile was set as follows: denaturation at 95 °C for 10 min; 45 cycles of denaturation at 95 °C for 10 s, annealing at 60 °C for 30 s, and extension at 72 °C for 1 s; and a final cooling step at 40 °C for 30 s. Samples were assayed experimentally in triplicate and then averaged to represent the data of a single experiment. Data was analyzed and quantified in LightCycler 480 software.

RNA-seq and bioinformatic analysis

Mouse cortices and hippocampi were collected for RNA extraction as described in the previous paragraph. RNA quality and quantifications were determined using an Agilent 2100 Bioanalyzer. The mRNA sequencing libraries were prepared using a Truseq Stranded mRNA kit (Illumina) and 75-76 cycle single-read sequencing was performed using the 500 High-output v2 (75 cycle) sequencing kit on an Illumina NextSeq500 instrument. Sequenced reads were trimmed for adaptor sequence and low quality sequences, and then mapped to the GRCm38.p6 whole genome using CLC Genomics Workbench (v.10.1.1, https://www.qiagenbioinformatics.com/) with parameters: mismatches = 2, minimum fraction length = 0.9, minimum fraction similarity = 0.9, and maximum hits per read = 5. Genes differentially expressed in WT mice with or without rotarod testing, and between *Tlr7*$^{-/Y}$ mice with or without rotarod testing were analyzed using CLC Genomics Workbench. The output data included fold-change, p-value, false discovery rate (FDR), total counts, RPKM and TPM. Differentially expressed genes (DEG) were defined by the criteria of fold-change > 1.3, a false discovery rate < 0.1 and average transcripts per million (TPM) > 0 (in each group). Protein networks and functional enrichments were analyzed using ingenuity pathway analysis (IPA) software and STRING (https://string-db.org/). Gene ontology biological processes were assessed using Metascape (http://metascape.org/gp/index.html). For heatmap analysis, TPM values of each gene was first normalized with the group of WT mice without rotarod testing and subjected to GraphPad Prism 8.0 for heatmap generation. The raw RNA-seq dataset has been available online (NCBI BioProject ID PRJNA702827).

BrdU injection, immunohistochemistry and quantification

After rotarod assays, mice received a single intraperitoneal injection of BrdU at a dosage of 150 mg/kg bodyweight for short-term labeling (**Figure 2A (3)**). For long-term labeling, a single intraperitoneal injection of BrdU was carried out each day for four consecutive days at a dosage of 100 mg/kg body weight. Experimental mice were anesthetized and perfused with 4% PFA in PBS. After 4% PFA postfixation at 4 °C, brains were sliced into 50-µm-thick sections using a vibratome. For IBA1 and GFAP staining, the brain sections were permeabilized with 0.3% Triton-X 100 in PBS for 10 min, then blocked for 30 min with blocking solution (0.2% bovine serum albumin, 0.3% horse serum and 0.3% Triton-X 100 in PBS). The sections were incubated overnight with IBA1 antibody (1:500; Wako, 019-019741) and GFAP antibody (1:500; Chemicon, MAB3402) in blocking solution at 4 °C. Sections were then incubated with Alexa Fluor-488- and Alexa Fluor-594-conjugated secondary antibodies (1:500) with DAPI for 3 h at room temperature. After mounting with antifade solution (0.5% N-propyl gallate, 20 mM Tris (pH8.0), 90% glyserol), the images were captured with an Axio imager M2 microscope (Carl Zeiss) equipped with a 20×/NA 0.80 (Plan-Apochromat; Zeiss) objective lens. Images were captured using a cooled charge-coupled device camera (Rolera EM-C2, QImaging) driven by the digital image processing software Zen Blue (Zeiss). The images were quantified using ImageJ (NIH). All images were converted into 8-bit format and adjusted (manually) with the threshold function, and the areas of CA3 and hilus regions of the hippocampus were analyzed. For BrdU staining, the sections were incubated with 0.3% H_2O_2 for 30 min and then washed three times with PBS. The slices were incubated in 2N HCl for 30 min at 37 °C for DNA hydrolysis and then neutralized with 0.1 M sodium borate buffer pH 8.5 for 10 min at room temperature. After washing three times with PBS, the sections were blocked with blocking solution (3% horse serum and 0.1% Triton-X 100 in TBS) for 30 min. The slices were incubated overnight with BrdU antibody (1:200; Abcam, ab6326), together with Dcx antibody (1:100; Santa Cruz, sc-8066) or NeuN antibody (1:100; Millipore, MAB377) in blocking solution at 4 °C. Sections were incubated with secondary antibodies plus DAPI and mounted as described above. The images were captured using a confocal microscope (LSM 700, Zeiss) equipped with a transmitted light detector (Zeiss LSM, T-PMT) and a 20x/NA 0.80 (Plan-Apochromat) objective lens. Quantifications were carried out in ImageJ software.

Statistical analysis

Data are presented as mean plus s.e.m. GraphPad Prism 8.0 was used for analyses and to generate plots. No statistical method was applied to evaluate sample sizes, but our sample sizes are similar to those of previous publications (Hung et al., 2018a; Hung et al., 2018b) and follow previously promoted principles (Charan and Kantharia, 2013). Statistical analyses were performed using two-tailed nonparametric tests (Mann-Whitney test) and two-way ANOVA with Bonferroni's test as indicated in the figure legends. *P* values < 0.05 were considered significant.

SUPPLEMENTAL REFERENCES

Charan, J., and Kantharia, N.D. (2013). How to calculate sample size in animal studies? Journal of pharmacology & pharmacotherapeutics *4*, 303-306.

Hsu, T.-T., Huang, T.-N., and Hsueh, Y.-P. (2020). Anterior Commissure Regulates Neuronal Activity of Amygdalae and Influences Locomotor Activity, Social Interaction and Fear Memory in Mice. Frontiers in molecular neuroscience *13*, 47.

Hu, H.T., Huang, T.N., and Hsueh, Y.P. (2020). KLHL17/Actinfilin, a brain-specific gene associated with infantile spasms and autism, regulates dendritic spine enlargement. J Biomed Sci *27*, 103.

Huang, T.N., Hsu, T.T., Lin, M.H., Chuang, H.C., Hu, H.T., Sun, C.P., Tao, M.H., Lin, J.Y., and Hsueh, Y.P. (2019). Interhemispheric Connectivity Potentiates the Basolateral Amygdalae and Regulates Social Interaction and Memory. Cell reports *29*, 34-48.e34.

Huang, T.N., Shih, Y.T., Lin, S.C., and Hsueh, Y.P. (2021). Social behaviors and contextual memory of Vcp mutant mice are sensitive to nutrition and can be ameliorated by amino acid supplementation. iScience *24*, 101949.

Hung, Y.F., Chen, C.Y., Li, W.C., Wang, T.F., and Hsueh, Y.P. (2018a). Tlr7 deletion alters expression profiles of genes related to neural function and regulates mouse behaviors and contextual memory. Brain Behav Immun *72*, 101-113.

Hung, Y.F., Chen, C.Y., Shih, Y.C., Liu, H.Y., Huang, C.M., and Hsueh, Y.P. (2018b). Endosomal TLR3, TLR7, and TLR8 control neuronal morphology through different transcriptional programs. J Cell Biol *217*, 2727-2742.

Kopf, M., Baumann, H., Freer, G., Freudenberg, M., Lamers, M., Kishimoto, T., Zinkernagel, R., Bluethmann, H., and Kohler, G. (1994). Impaired immune and acute-phase responses in interleukin-6-deficient mice. Nature *368*, 339-342.

Lin, C.W., and Hsueh, Y.P. (2014). Sarm1, a neuronal inflammatory regulator, controls social interaction, associative memory and cognitive flexibility in mice. Brain Behav Immun *37*, 142-151.

Liu, H.-Y., Hung, Y.-F., Lin, H.-R., T.-L., Y., and Hsueh, Y.-P. (2017). Tlr7 Deletion Selectively Ameliorates Spatial Learning but does not Influence Aβ Deposition and Inflammatory Response in an Alzheimer's Disease Mouse Model. Neuropsychiatry *7*, 509-521.

Lund, J.M., Alexopoulou, L., Sato, A., Karow, M., Adams, N.C., Gale, N.W., Iwasaki, A., and Flavell, R.A. (2004). Recognition of single-stranded RNA viruses by Toll-like receptor 7. Proc Natl Acad Sci U S A *101*, 5598-5603.

Shih, P.Y., Hsieh, B.Y., Lin, M.H., Huang, T.N., Tsai, C.Y., Pong, W.L., Lee, S.P., and Hsueh, Y.P. (2020a). CTTNBP2 Controls Synaptic Expression of Zinc-Related Autism-

Associated Proteins and Regulates Synapse Formation and Autism-like Behaviors. Cell reports *31*, 107700.

Shih, P.Y., Hsieh, B.Y., Tsai, C.Y., Lo, C.A., Chen, B.E., and Hsueh, Y.P. (2020b). Autism-linked mutations of CTTNBP2 reduce social interaction and impair dendritic spine formation via diverse mechanisms. Acta neuropathologica communications *8*, 185.

Wu, P.J., Hung, Y.F., Liu, H.Y., and Hsueh, Y.P. (2017). Deletion of the Inflammasome Sensor Aim2 Mitigates Abeta Deposition and Microglial Activation but Increases Inflammatory Cytokine Expression in an Alzheimer Disease Mouse Model. Neuroimmunomodulation *24*, 29-39.